PROTOLITH AND METAMORPHIC CONDITIONS OF THE METAPELITES FROM THE RIO CLARO REGION (ANTIOQUIA DEPARTMENT)

Author

DIANA CAROLINA MADRID RESTREPO

201610012015

Supervisor

CAMILO BUSTAMANTE LONDOÑO

Department of Earth Sciences

School of Sciences

EAFIT University

Medellín

2021

Contents

List of figures

List of Tables

1.**Abstract**

The Cajamarca Complex is distributed along the Central Cordillera of Colombia, its formation is attributed to a Permian subduction zone, volcanic arc magmatism, opening and closing of basins and accretion of terrenes. The 16 samples studied in this research crop out near Rio Claro in the department of Antioquia. The analyzes were made with 7 metasedimentary, 2 metabasic belonging to the Cajamarca Complex and 7 pegmatites related to the magmatism of the Antioquia Batholith. Detailed petrography of the samples was performed and did total rock geochemistry for metamorphic rocks for analysis of major and trace elements. This study focuses on discussing the tectonic environment of protolith formation based on tectonic discrimination diagrams and P-T conditions for metamorphism, based on mineralogical reactions. In the N-MORB analysis it shows an enrichment in the LILE and a depleting in the HFSE, in the same way an inverse relationship is observed of the rare earth elements (REE) normalized with the primitive mantle. The metasedimentary rocks are mainly formed by quartz, muscovite, biotite, graphite, Andalusite and as accessory minerals titanite and zircon; the metabasics are composed of epidote, actinolite, chlorite, hornblende, and plagioclase. The P-T conditions yields a pressure of 6 to 4 kbar and a temperature that did not exceed 550 ° C. This represents a metamorphic gradient of medium pressure and medium temperature indicating a passage through the green schist to epidote-amphibolite facies which is linked to a Barrovian type metamorphism. This type of regional metamorphism led toward a depth approximately of 20 km. In this work it is suggested that the formation of the sedimentary protolith is in the accretion wedge of a subduction zone, unlike the igneous protolith that would be part of the formation of the crust. oceanic; this differs from what Blanco-Quintero et al. (2014) proposes south of the Cajamarca Complex. This oceanic crust would later subduct to the paleo western margin of South America; where the metamorphic event would finally be generated.

1. Introduction

Northwestern South America records the formation of the supercontinent Pangea during the Permian, its fragmentation during the Triassic and the opening of the proto-Caribbean ocean (Spikings, 2019). In this way, the tectonics of NW South America during the late Paleozoic

to Triassic have implications to understand the interaction between Laurentia and Gondwana that were part of the supercontinent and the origin of several tectonostratigraphic terrains that were dispersed by the breaking of this supercontinent by the end of the Triassic (Cardona et al.,2009; Correa et al. (2020).

The igneous and metamorphic rocks formed during this time interval have been attributed to a Permian continental arc setting that was active between ca. 288 and 264 Ma as seen by U-Pb crystallization ages in zircons (Cochrane et al.,2014; Cardona et al., 2009; Cardona et al., 2010b; Rodriguez et al., 2017). The igneous rocks are intruding an amphibolite facies Paleozoic metamorphic basement in the Central Cordillera (Cardona-Molina et al., 2006), whose origin is attributed to the subduction of the proto-Pacific plate on the western margin of Pangea (Keppie et al., 2008; Nance et al., 2012). Other known models consider that the Permian rocks were formed in a continental arc followed by anatexis during the Triassic (Spikings et al.,2015) and/or a post-collisional anatectic event that formed the granites at 280 Ma (Piraquive, 2017) and 228 Ma (Vinasco et al., 2006).

The Central Cordillera records a tectonic evolution where subduction, volcanic arc magmatism, opening and closure of sedimentary basins, and terrane accretions are identified from the Permian to the present (Restrepo and Toussaint, 1982,1988; Bayona et al., 2006; Vinasco et al., 2006; Kennan and Pindell, 2009). The lithological record of these events consists of I-type granites, migmatites and amphibolites (Vinasco et al., 2006; Cochrane et al., 2014; Spikings et al., 2015) grouped in the Cajamarca Complex (Maya and González, 1995); this complex also includes quartz-sericitic schists, green schists, phyllites, quartzites and marbles (Mosquera et al., 1982).

In this work, we present detailed petrographical descriptions together with whole rock geochemistry of quartzites, micashists and amphibolites that crops-out at the eastern flank of the Central Cordillera (Antioquia department; **Figure 1**). The results aim to determine the metamorphic conditions, the origin of their protoliths and identify possible correlations.

2. Generalities

3.1 Question

Is the formation of the protoliths and the metamorphic event that formed the Cajamarca Complex correlated throughout its N-S extension in the Central Cordillera**?**

3.2 Hipotesis

The metamorphic rocks of the Cajamarca Complex to the north of the Central Cordillera can be correlated with those of the south in the generation of the metamorphic event, but they are not correlated in the formation of the igneous and sedimentary protolith.

3.3 General objective.

Evaluate the formation environment of the protoliths of the metasedimentary and metabasic rocks belonging to the Cajamarca Complex together with the metamorphism event to the north of the Central Cordillera, to correlate them or not with the metamorphic rocks described to the south of the mountain chain and to be able to infer the timing of the events.

3.4 Specific objetives.

- Determine metamorphic conditions from pressure and temperature paths based on the mineralogy obtained, observed textures and metamorphic reactions.
- To be able to contribute to the understanding of the tectonic environment in which the metabasic and metaedimentary rocks were formed.
- -Make a temporal correlation to infer ages of possible protolith formation events and the metamorphic event.

4 Geological setting

The Andes in Colombia are divided into three mountain ranges: The Eastern, Central and Western Cordilleras. The Eastern Cordillera comprises a basement composed of Precambrian and Paleozoic metamorphic rocks (gneiss, granulites and amphibolites) and Ordovician to Silurian granitoid rocks. This basement is covered by Paleozoic to Mesozoic sedimentary sequences (Kroonenberg 1982; Restrepo-Pace et al. 1997; Cordani et al. 2005; Sarmiento-Rojas et al., 2006; Horton et al., 2010; Cardona-Molina et al., 2006; Ordóñez-Carmona et al., 2006; van der Lelij et al., 2016; González et al.1988). The Western Cordillera comprises allochthonous oceanic plateau-related rocks that accreted to the continental margin since the late Cretaceous (Kerr et al. 1997; Villagómez et al. 2011) and volcanic arc sequences composed of basic volcanic rocks and marine sediments from the upper Cretaceous and Cenozoic intruded and covered by Cenozoic igneous rocks and volcanic sequences (Aspden et al. 1987; González et al. 1988; Kerr et al. 1997; Kerr and Tarney 2005; Villagómez et al. 2011).

The Central Cordillera, in which the studied area is located, consists of Paleozoic to Cretaceous metamorphic rocks of variable grade and intruded by Jurassic to Paleogene volcanic arc-related plutonic rocks (Restrepo and Toussaint 1982; Aspden et al. 1987; Maya

and González 1995; Bayona et al. 2012). The eastern flank of the Central Cordillera includes I-type granitoids, migmatites and amphibolites (Vinasco et al. 2006; Cochrane et al. 2014a; Spikings et al. 2015) grouped in the locally known Cajamarca Complex. This complex includes pelitic schists, quartzites, marbles and amphibolites (Ardila,1986; González, 2001; Correa and Martens, 2000), and are intruded by Triassic S-type granitoids and volcano-sedimentary rocks (Vinasco et al. 2006; Restrepo et al. 2011; Cochrane et al.2014a; Aspden et al.1987).

4.1 Geology of the study area

The studied area is located southeast of the Antioquia department, on the eastern flank of the Central Cordillera (**Figure 1**). It consists mainly of quartz-muscovite schists where large outcrops are present in the rivers of the area as Rio Claro and Norcasia, in a narrow strip of more than 25 km long and less than 1 km wide between the Palestina and Cocorná Sur faults (**Figure 2**) (Feinniger et al.1972). The rocks of this region include fine-muscovite, quartz, biotite and graphite. Quartzites are the second most abundant rock. The best outcrops are in small valleys south of Amalfi, La Gómez and Montaña valleys and tributary of the Rio Claro (Feiniger et al.1972), the protoliths of these units vary from sand to silt and from quartz sand and silt shale. Feldspathic gneisses also occur in the area; the outcrops occur near to the Palestine Fault. In this unit is characteristic of andalusite porphyroblasts partially or totally replaced by fine muscovite, outcrops are found on the Rio Claro between the Jetudo and Palestina Faults. Marbles occur to the east of the Palestina Fault; all the bodies are interspersed with the quartz-sericitic schists (González, 1980; Feininger et al. 1972), the marbles are mainly composed of carbonates and as accessory minerals quartz, graphite, micas, pyrite and white mica (González, 1980; Feininger et al. 1972)

Amphibolites crops between the Palestina and Mulato Faults, and between the Palestina and Jetudo Faults (**Figure 2**). This rock consists in a 90% of hornblende and plagioclase and as accessory and alteration mineral are epidote and chlorite. Finally, greenschists crops out in the Arma and Sonsón rivers, and the highway Sonsón-Arma river. This rock consists of actinolite, epidote/zoisite, chlorite, quartz and plagioclase.

The igneous rocks present in the study area are part of the Antioquia Batholith, the best outcrops are found in the Santo Domingo and Cocorná rivers and in the El Biadal creek, tributary streams of the Nus, Guatapé and San Carlos river. The Antioquia Batholith is the only late Cretaceous intrusive body recorded in the Cordillera Central and constitutes the first record of continental arc magmatism in NW South America after 20 m.y. of magmatic quiescence (Bustamante et al., 2016; Duque-Trujillo et al., 2019). The age of crystallization according to U-Pb ages in zircons is between 97 and 58 Ma (Duque-Trujillo et al., 2019 and references there in). Compositionally it varies from granodiorite to tonalite (Feiniger et

al.,1972 and Botero, 1982)

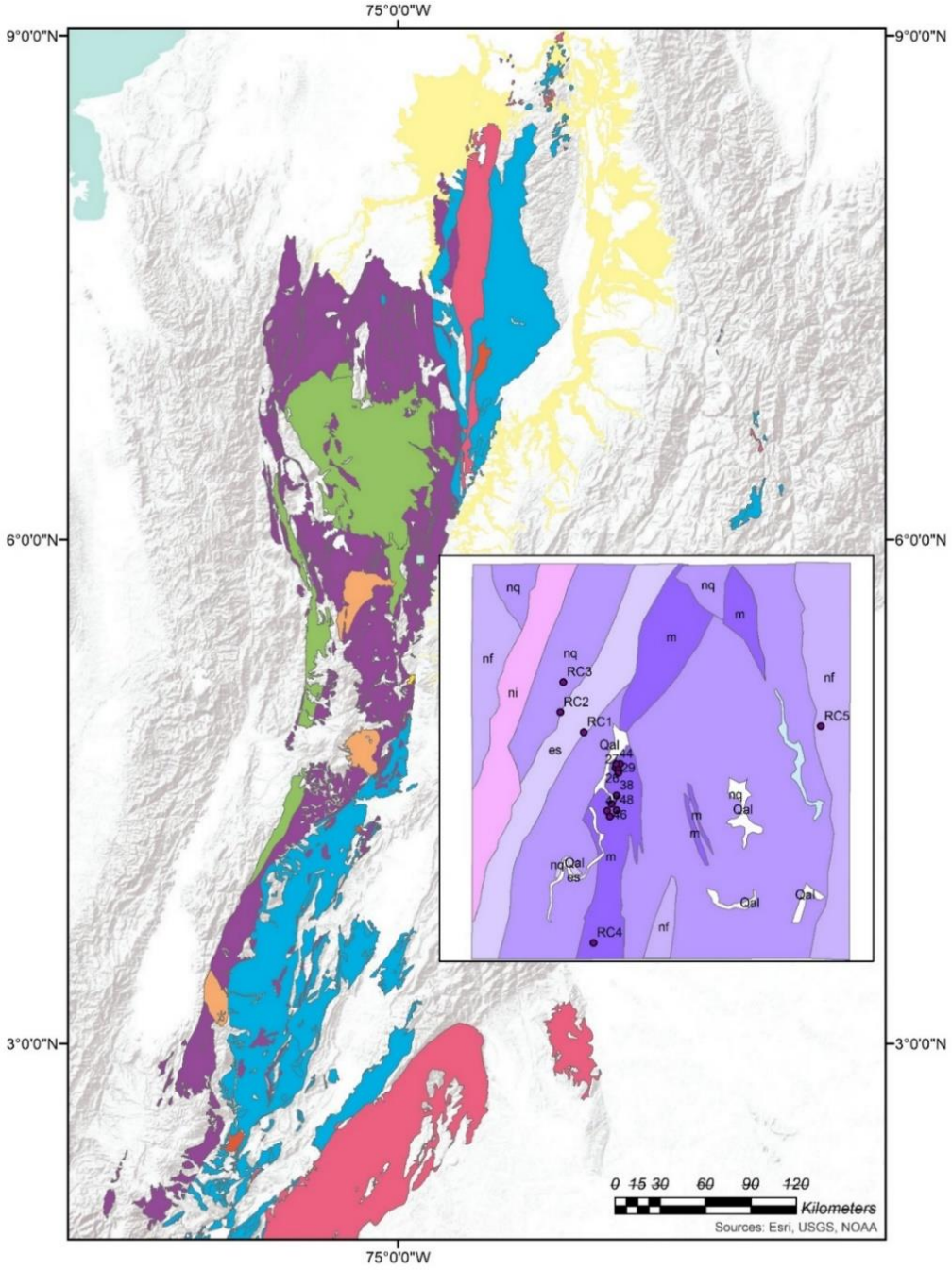

Figure 1: Localization and geology of area's study with samples plotted

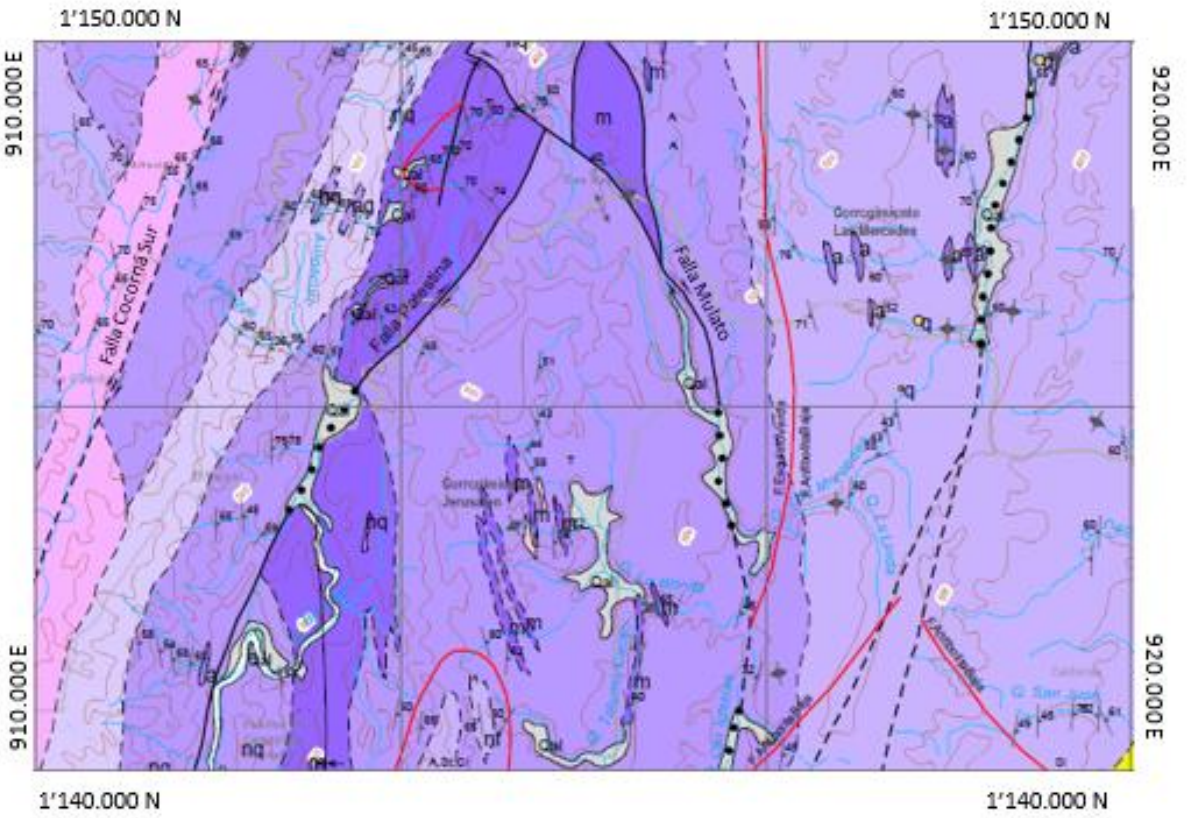

Figure 2: Geology of the area bounded by the faults Cocorná Sur to the west, Palestina to the middle and Mulato fault to the east.

5 Analytical techniques

This Project was made to discuss about of the formation environment of the protolith and metamorphic event of the rocks of the Cajamarca Complex north of the Central Cordillera, for this, pressure and temperature conditions were inferred and to be able to conclude which environment was dominating at that time based on in a detailed petrographic study of the metamorphic rocks found there, also, define their relationship with igneous rocks and their high cataclastic deformation. To carry out this purpose, 16 samples were collected, 7 meta-sedimentary rocks, 2 metaigneas and 7 igneous rocks in the southwest of the department of

Antioquia in the eastern flank of the Central Cordillera, in the jurisdiction of the municipality of Sonsón, Jerusalem district, Río Claro area.

5.1 Petrography

Detailed petrography was performed on the thin sections in the Geology laboratory of the EAFIT University, the Leitz microscope was used and photographs were taken to recognize textures and alterations, based on this, the metamorphic reactions seen in the petrography were defined based on the book Petrogenesis of Metamorphic Rocks 6th edition (Butcher & Frey, 1994) and finally the trajectories of P- T were made for both metaigneous and metaedimentary in order to infer metamorphic conditions (pressure and temperature) and thus have an approximation of the geological environment

5.2 Whole rock geochemistry

Mayor oxides and trace elements concentrations were determined for 10 samples by X-ray fluorescence (XRF) and inductively coupled plasma-mass spectrometry (ICP-MS) at ALS Minerals. The samples were crushed using a jaw crusher and powered using a tungsten carbide ring mill. The powered samples (0.2 g) were weighed into a graphite crucible and mixed with 1.5 g of LiBO2 flux. The crucibles were heated in a furnace to 1050°C for 15 minutes, and the resulting melt was dissolved in 5% HNO3. Calibration standards and reagent blanks were added to the sample sequence. Sample solutions were aspirated into an ICP emission spectrograph (Jarrel Ash Atom Comb 975) for determining major oxides and certain trace elements (Ba, Nb, Ni, Sr, Sc, Y, and Zr), while the sample solutions are aspirated into an ICP-MS (Perkin-Elmer Elan 6000) for determination of the trace elements, including rare earth elements. All geochemical analyses *were* handled and processed using the software

GCDKit, 5.0 (Janoušek et al., 2006). The results for the metasedimentary rocks are included in table 1 and for the metabasic rocks in table 2.

Table 1 Geochemical of metasedimentary rocks of the region rio claro

SAMPLE	RC-25-34	RC-26-37	RC-29-66	RC-27-62		RC-25-33	RC-2	RC-3	RC-4
Ba	716	2240	1475	5300		750	106,5	1000	13,2
Ce	112	76,3	82,1	68,3		124,5	34,4	50,6	1,5
Cr	120	120	140	100		110	20	80	20
Cs	15,8	10,15	18,95	8,19		11,3	0,52	6,9	4,42
Dy	7,81	4,94	6,57	4,44		8,61	2,49	4,24	0,2
Er	4,5	2,84	3,77	2,98		4,98	1,38	2,47	0,16
Eu	1,78	1,32	1,43	1,08		2,25	0,57	0,98	0,03
Ga	35,1	29,1	27,9	26,5		33,7	4,9	22,5	0,8
Gd	7,91	5,35	6,78	4,4		9,31	2,48	4,46	0,26
Hf	5,7	5,5	6	3,9		5,2	5,9	5,5	0,2
Ho	1,61	0,97	1,35	0,93		1,75	0,42	0,86	0,07
La	53,6	37,6	38,9	30,5		58,8	19,6	24	2,2
Lu	0,69	0,45	0,57	0,47		0,65	0,18	0,42	0,02
Nb	22,5	16,2	18,2	16,5		21,7	13,3	10,3	0,3
Nd	49,7	34,4	38,8	28,7		57,6	16,4	23,7	1,4
Pr	12,8	9,08	9,63	7,35		14,35	4,61	6,14	0,34
Rb	237	118	170,5	111,5		148,5	14,9	121	23,4
Sm	9,28	6,77	7,46	5,43		11,1	2,88	4,48	0,15
Sn	8	5	5	4		7	1	2	1
Sr	147,5	100,5	51	26		137	16,7	249	135,5
Ta	1,8	1,5	1,6	1,4		1,8	0,8	0,8	0,1
Tb	1,35	0,83	1,09	0,68		1,49	0,41	0,72	0,04
Th	20,6	13,25	13,55	12,7		20,1	3,55	8,82	0,18
Tm	0,7	0,41	0,59	0,46		0,72	0,16	0,4	0,03
U	4,22	4,91	3,42	2		3,38	1,12	2,06	0,42
V	199	171	179	146		168	20	113	11
W	4	9	8	5		4	2	2	2
Y	39,8	22,7	32,4	22,6		43,1	12,6	23	2,8
Yb	4,37	2,94	3,91	2,96		4,44	1,37	2,51	0,14
Zr	204	204	227	145		184	240	205	8
SiO2	52,4	60,1	59,5	64,6		54,1	93,9	68,1	81,5

Al2O3	22,4	17,45	17,55	14,95		20,4	3,55	15,05	0,4
Fe2O3	8,47	6,69	7,82	7,44		9,22	1,08	5,11	0,36
CaO	0,52	1,54	1,29	0,54		0,75	0,07	1,05	10,1
MgO	1,99	2,7	2,77	2,9		2,07	0,19	1,79	0,43
Na2O	1,44	2,65	1,91	0,6		1,98	0,41	2,58	0,02
K2O	4,57	3,09	4,69	3,37		3,5	0,34	2,55	0,13
Cr2O3	0,015	0,016	0,017	0,012		0,014	0,002	0,01	0,002
TiO2	0,97	0,79	0,95	0,74		0,94	0,16	0,67	0,02
MnO	0,1	0,06	0,05	0,15		0,1	0,02	0,06	0,01
P2O5	0,16	0,17	0,21	0,06		0,19	0,08	0,16	<0.01
SrO	0,02	0,01	0,01	<0.01		0,02	<0.01	0,02	0,01
BaO	0,08	0,26	0,17	0,6		0,08	0,01	0,11	<0.01
LOI	5,82	4,05	2,69	3,29		5,08	1,61	3,15	8,82
Total	98,96	99,58	99,63	99,25		98,44	101,42	100,41	101,8
As	5	36	6	286		<5	12	52	<5
Co	22	12	15	15		23	2	3	1
Cu	41	34	25	53		53	3	29	1
Li	230	270	530	210		240	10	40	140
Mo	1	<1	<1	<1		1	<1	1	1
Ni	48	35	40	62		46	2	13	3
Pb	28	16	15	12		34	5	21	3
Sc	22	14	18	18		20	2	14	<1
Zn	135	146	132	159		125	17	57	11

Table 2 geochemical of metabasic rocks of the region rio claro

SAMPLE	RC-1	RC-5
Ba	389	66,1
Ce	51,4	29,1
Cr	60	160
Cs	1,64	0,33
Dy	4,85	9,47
Er	2,88	4,71
Eu	1,14	2,47
Ga	16,7	25,1
Gd	5,56	9,37
Hf	5,6	4,9
Ho	1,03	1,77

La	27,7	14,9
Lu	0,37	0,57
Nb	9,8	11,3
Nd	27	29,2
Pr	6,95	5,6
Rb	39,9	6,5
Sm	5,08	7,7
Sn	2	2
Sr	269	244
Ta	0,8	0,7
Tb	0,84	1,51
Th	9,13	0,77
Tm	0,4	0,66
U	2,26	0,08
V	107	437
W	4	2
Y	28	48,8
Yb	2,48	3,8
Zr	210	172
SiO2	69,6	43,6
Al2O3	13,85	14,25
Fe2O3	5,22	16,1
CaO	2,99	9,5
MgO	2,03	7,59
Na2O	3,18	2,47
K2O	0,65	0,44
Cr2O3	0,009	0,021
TiO2	0,66	2,73
MnO	0,09	0,24
P2O5	0,16	0,14
SrO	0,02	0,02
BaO	0,04	0,01
LOI	2,39	2,34
Total	100,89	99,45
As	12	<5
Co	10	52
Cu	36	137
Li	70	20

Mo	<1	1
Ni	19	97
Pb	20	2
Sc	13	39
Zn	78	153

6 Results

6.1 Petrography

The studied area is composed of metamorphic and igneous rocks. The metamorphic rocks analyzed in this research were divided into two groups, and based on the petrographic characteristics, and their protoliths were interpreted as sedimentary (samples RC2, RC3, RC4, 2637, 444, 1254, 2966) and igneous, probably basic in composition (samples RC1 and RC5). Deformation, replacement, mineralogy, and rock classification characteristics will be presented below:

The metasedimentary rocks are mainly made up of quartz (20-50%), muscovite (30-40%), biotite (9-40%) and graphite (10-13). In the table 3 are the classification of metasedimentary rocks following Bucher and Frey (1994).

Table 3. Classification of metasedimentary rocks of the studied area following Bucher and Frey (1994) ´s book.

SAMPLE	RC-25-34	RC-26-37	RC-29-66	4441	RC-2	RC-3	RC-4
Quartz	7%	50%	40%	20%	30%	30%	85%
Muscovite	40%	10%	10%	30%	24%	45%	85%
Biotite		40%	40%	40%	20%	9%	
Plagioclase					1%		
Graphite	13%		15%	10%		10%	
K-feldspar						6%	
Hornblende					2%		

Titanite					2%		
Zircon					1%		
Carbonates							10%
Andalusite	30%						
Chlorite	10%						
Zone	Andalusite	Biotite	Biotite	Biotite	Biotite	Biotite	
Facies	Epiodte-amphibolite facies	Greenschist facies	Greenschist facies	Greenschist facies	Greenschist facies	Greenschist facies	
Name	Graphite-Andalusite-Muscovite schist	Muscovite-Biotite-Quartz schist	Graphite-Biotite-Quartz schist	Graphite-Muscovite-Biotite schist	Biotite-Muscovite-Quartz Schist	Graphite-Muscovite-Quartz Schist	Cuarcita

Quartz a grain size varies from 0.1 to 0.2 mm, is usually subidioblastic to xenoblastic and has interlobed contacts and polygonal mosaic texture (Figure 3). Together with biotite, muscovite and graphite this mineral defines the grain-lepidoblastic texture and S_1 (Figure 4); in the sample RC3, quartz is pre-S_1 (Figure 5). Another, common observed pattern is the undulatory extinction of quartz.

Muscovite crystal size varies from 0.3 mm to 1.0 mm approximately. This mineral is in general idioblastic to subidioblastic and is defining the grano-lepidoblastic texture and S_1 (Figure 4). This mineral also defines crenulation cleavage (Figure 6).

Biotite has a crystal size varying between 0.1 mm to 0.6 mm approximately. The crystals are commonly subidioblastic and defines a lepidoblastic texture, and S_1 foliation (Figure 4), and is found along the crenulation cleavage of sample 2638 (Figure 7). Exceptionally, sample 2966 exhibit biotite pos-S_1 (Figure 8).

Graphite presents a granulometry of 0.4 mm and defines with the other minerals the foliation S_1.

There is presence of **andalusite** porphyroblasts (30%), with grains of 4mm, it is completely replaced by muscovite (Figure 9) and possibly correspond to S_1; event.

Accessory minerals are **chlorite** (10%) pos-kinematic at S_1 (Figure 10). **Hornblende** were found in sample RC2 and its grain size varies from 0.1 to 0.4mm (Figure 11). **Titanite** and **zircons** are observed in sample RC2.

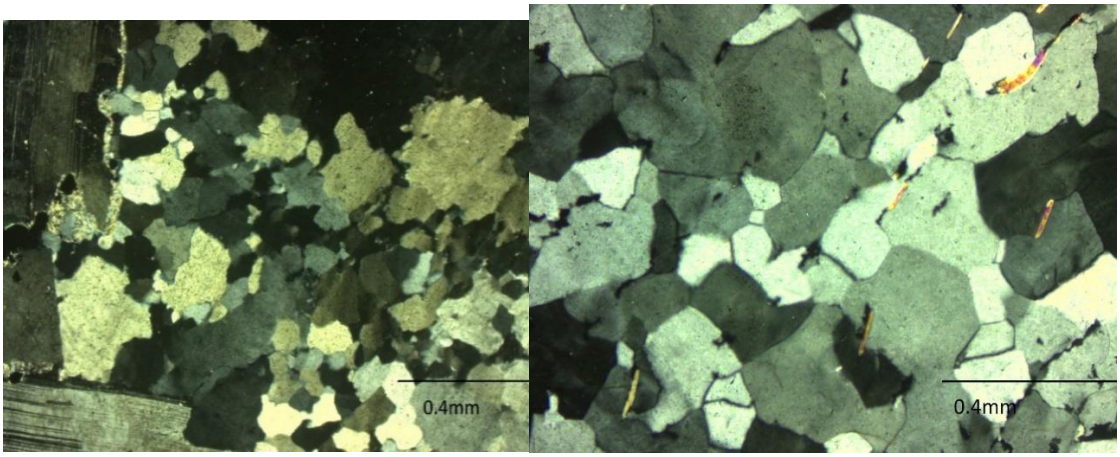

Figure 3 Quartz's textures "interlocking" (left, section 2749), polygonal mosaic (right, section RC4) images obtained with cross polarized light (XPL)

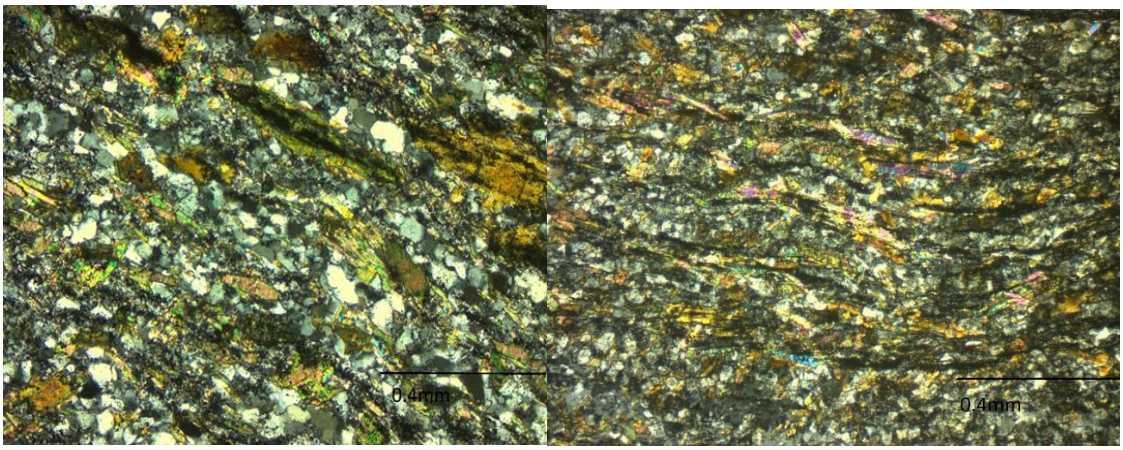

Figure 4. Texture grano-lepidoblastic, conformed by muscovite, biotite and graphite. Section 2966 (left), section 4441 (right). Images obtained with XPL

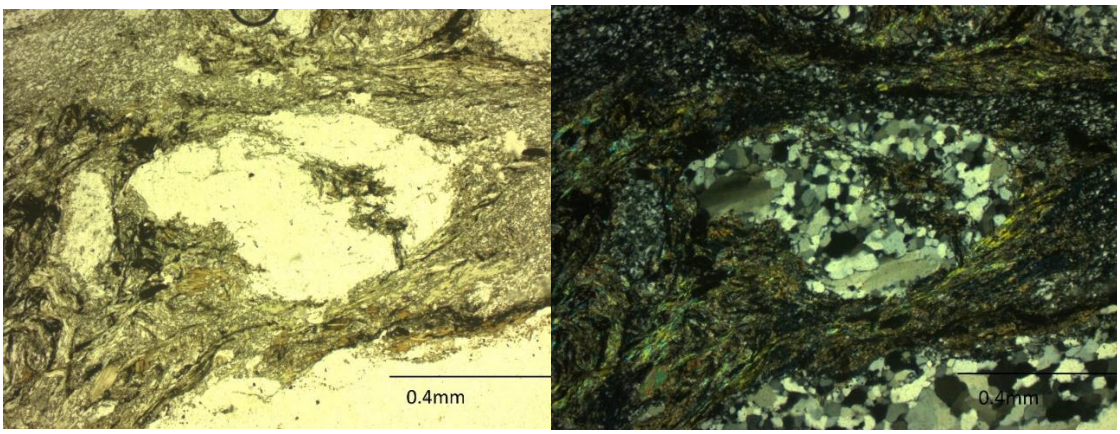

Figure 5. Quartz pre-S1; Section RC3. In plane polarized light (PPL -left) XPL-right.

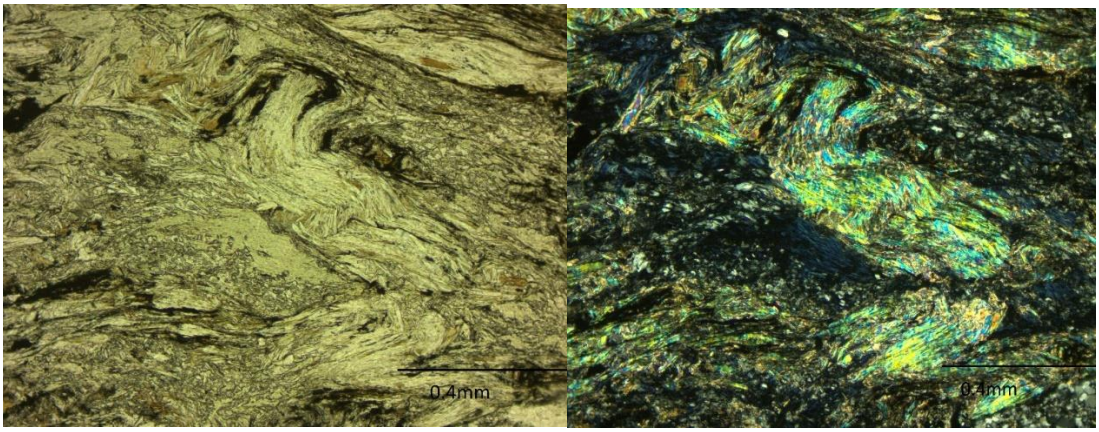

Figure 6 crenulation cleavage in the section RC3. PPL (left) and XPL (right).

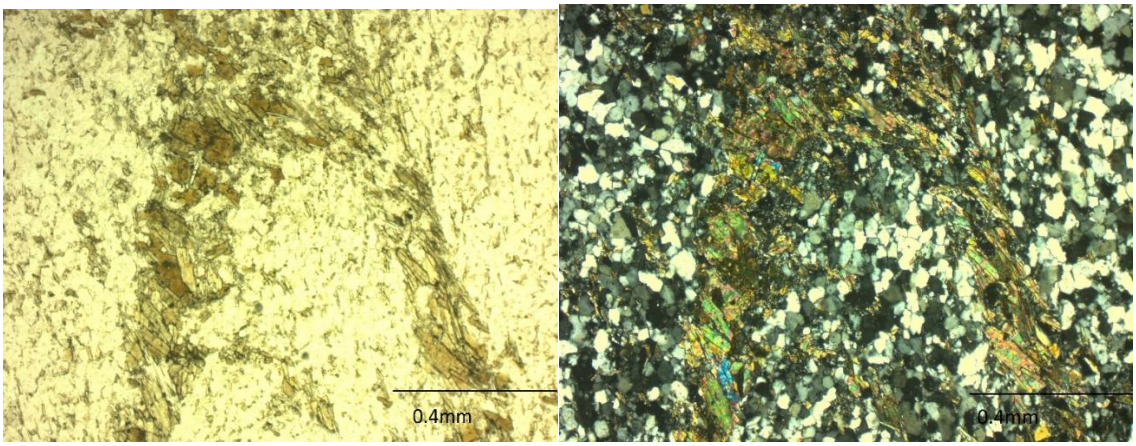

Figure 7 crenulation cleavage defined by biotite. Section 2638, PPL (left) XPL (right).

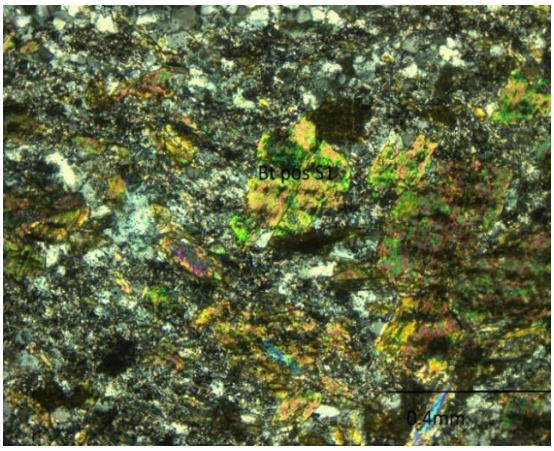

Figure 8 Biotite pos-S1 in sample 2966 XPL

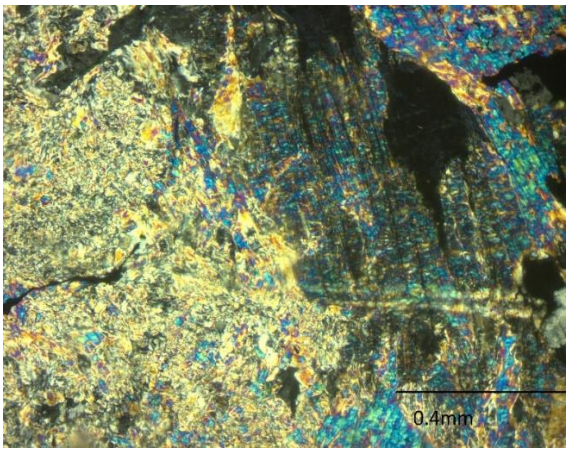

Figure 9. Muscovite after andalusite, sample 2534, XPL

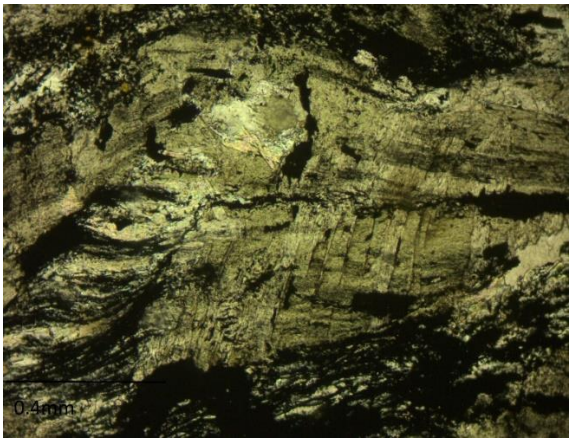

Figure 10 Chlorite pos-kinematic S_1 in sample 2534 PPL

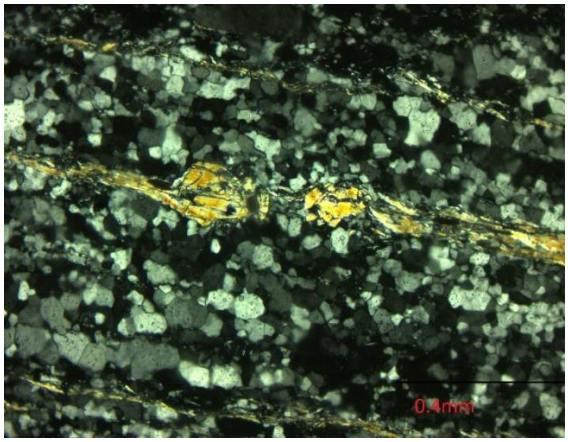

Figure 11. Relict of hornblende prior to S_1 in sample RC2 XPL

Table 4. Classification of metabsic rocks of the studied area following Bucher and Frey (1994).

SAMPLE	RC-1	RC-5
Plagioclase	5%	20%
Epidote	10%	10%
Hornblende		70%
Actinolite	75%	
Quartz	3%	
Chorite	7%	

Facies	Greenschist facies	Greenschist facies
Name	Esquisto Verde	Anfibolita

Metabasic rocks found in the area correspond to samples RC1 and RC5. Both samples exhibit several differences as follow:

The sample RC1, is made up of **actinolite** (75%), **epidote** (10%), **chlorite** (7%), **plagioclase** (5%) and **quartz** (3%).

Actinolite grains are less than 0.3mm, idioblastic and defines grano-nematoblastic texture and S_1; **epidote** is xenoblastic, pre-kinematic also this mineral is zoned, (Figure 12) and syn-kinematic (Figure 13) and **chlorite** has a size 0.6mm, **plagioclase** is less 0.2mm and **quartz** is less 0.3mm approximately. All minerals in this section are defining S_1.

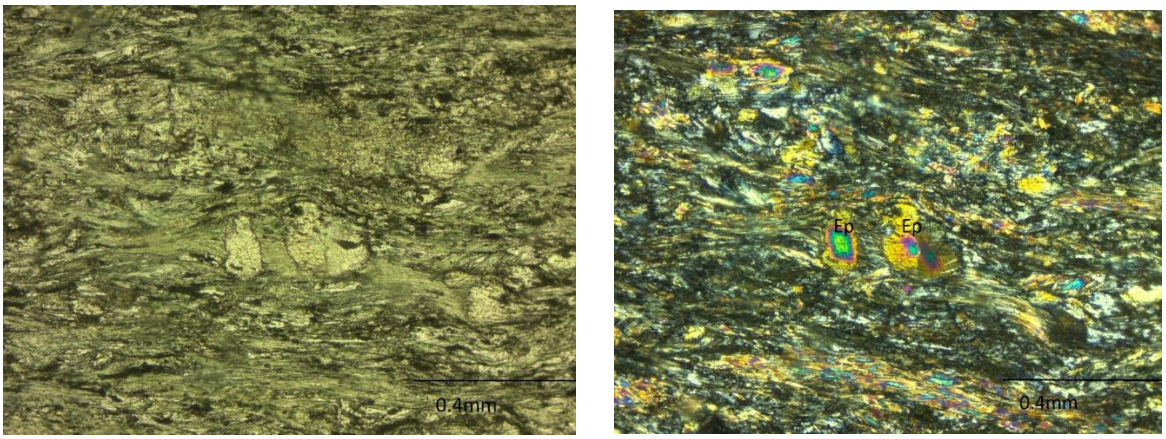

Figure 12; Section RC1, epidote pre-kinematic to S1 and zonation. PPL (left) and XPL (right).

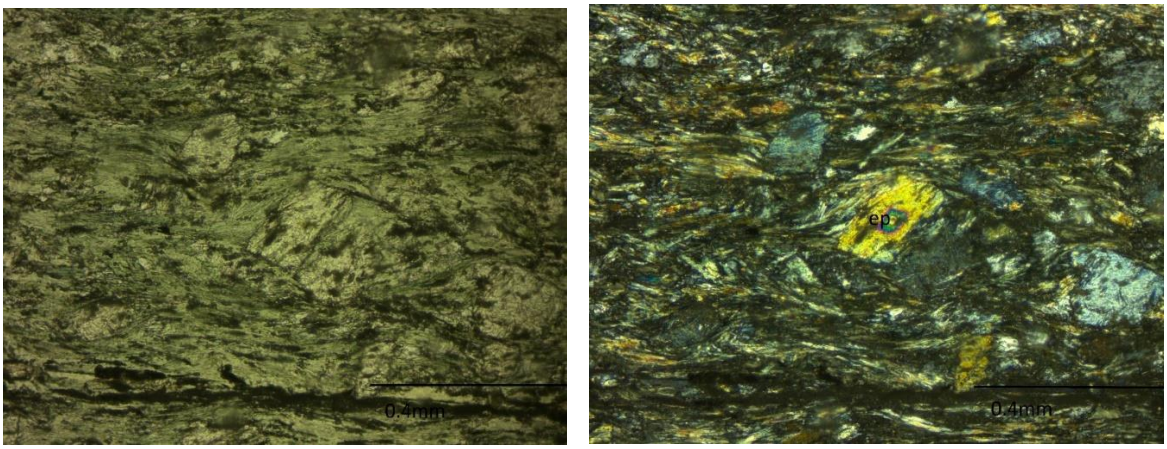

Figure 13; Section RC1, epidote syn-kinematic. In PPL (left) and XPL (right).

The sample RC5, is made up of **hornblende** (70%), **plagioclase** (20%), **epidote** (10%)

The **plagioclase** has a granulometry of 0.7 mm to 1.3 mm approximately, is subidioblastic and is partially replaced by epidote and muscovite (Figure 14 and Figures 16,17) and finally the epidote has a size less to 0.4 mm.

The **hornblende** has a size of 0.5 mm-1.7 mm. This mineral is idioblastic to subidioblastic and is partially replaced to epidote (Figure 15).

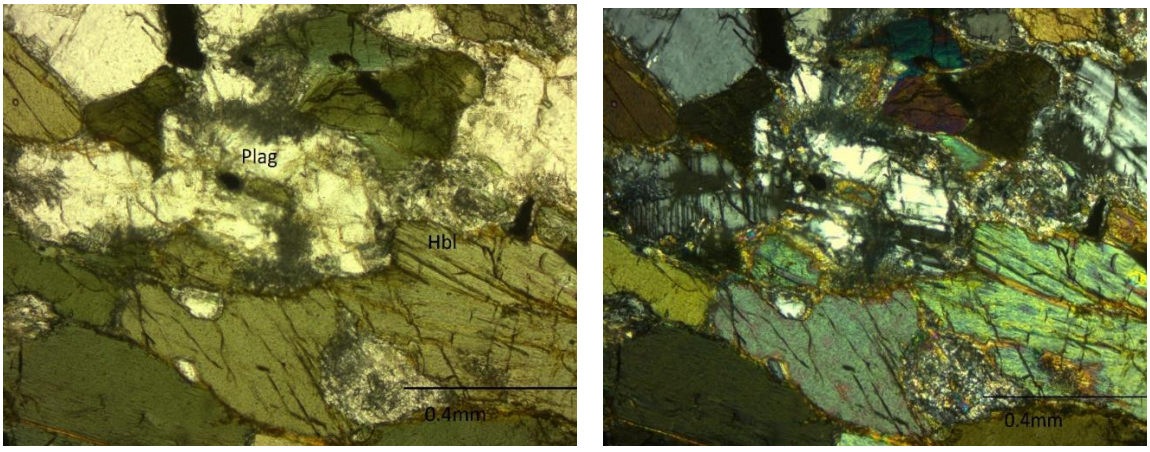

Figure 14. Plagioclase (Plag) grains partially replaced at the edges by muscovite, is in association with hornblende (Hbl). Section RC5, PPL left, XPL right.

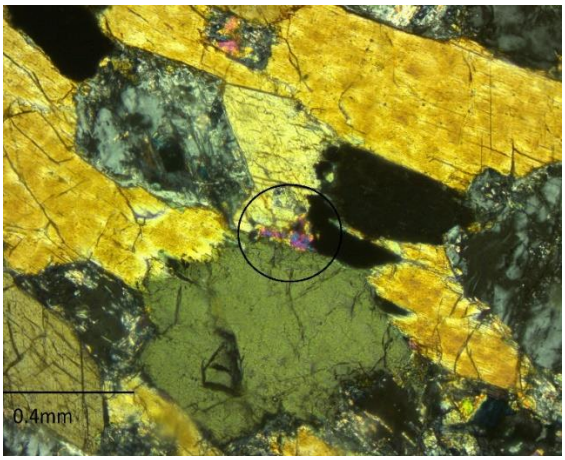

Figure 15. Epidote after hornblende, obtain-Ned XPL

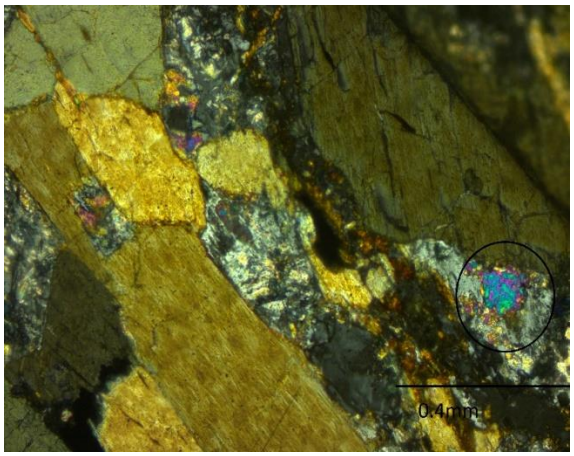

Figure 16. Epidote after plagioclase, image obtained with XPL.

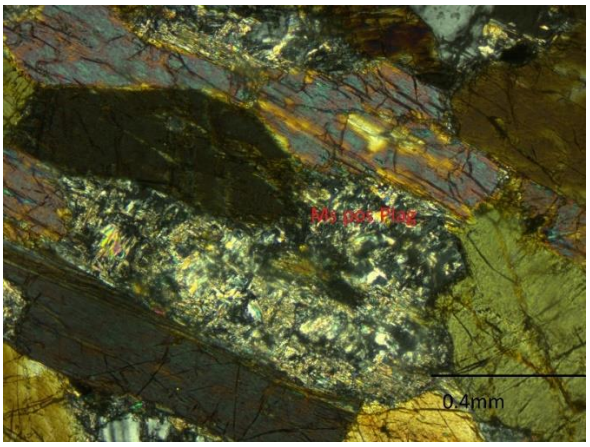

Figure 17. Section RC5, Fine muscovite after plagioclase in association with hornblende.

A blastesis diagram was obtained in order to synthesize relationship between mineral growth and foliation planes S_1 (Figures 18 y 19)

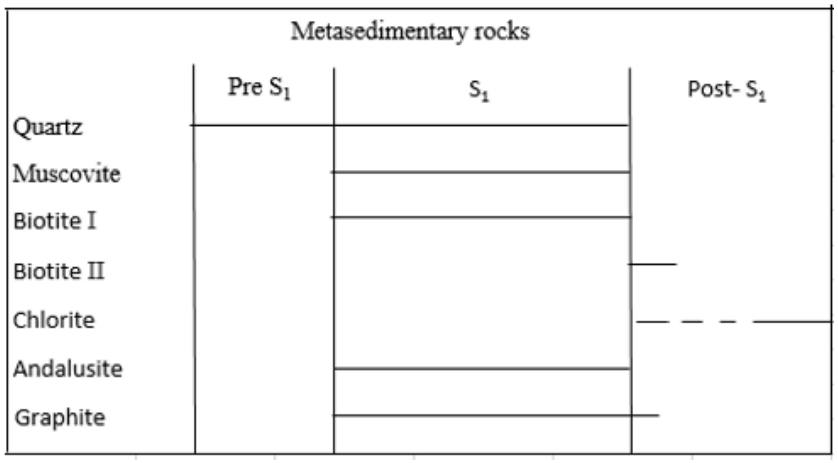

Figure 18 Blastesis of metasedimentary rocks

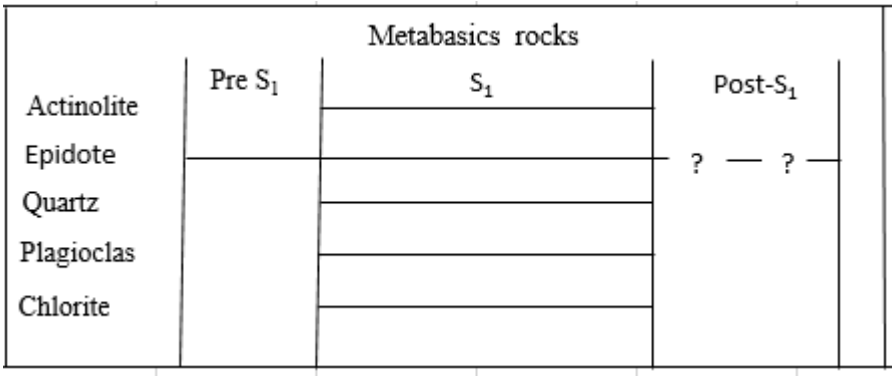

Figure 19: Blastesis of metabasic rocks

6.3 Geochemical

The metasedimentary and metabasic samples were used to perform an analysis of major elements and trace elements, in order to observe behaviors in the graphs, geotectonic classification, etc., and thus sustain the tectonic conditions that dominated the study area.

The Geochemistry of these rocks serves as an indicator of their formation environment, using the High Field Strength Elements (HFSE) and the Rare Earth Elements (REE) since these are the most reliable tracers for petrogenetic interpretations, unlike the Large Ion. Lithopile Elements (LILE) and some major elements (Na, K, Ca, Mg, Rb, Ba, Sr) that are susceptible to being removed during deposition and metamorphism processes (Michard, 1989; Wilson, 1989; Rollinson, 1993, Hollings and Wymann, 2005; Winchester and Floyd, 1977; Pearce, 1982; Jenner, 1996).

6.3.1 Geochemical of metasedimentary rocks

8 samples were used for major and trace element analysis. Although total rock geochemistry is normally used in igneous rocks to identify patterns that can be associated with a specific

tectonic environment (Rollinson, 1993), the geochemical composition of sediments or their metamorphic equivalent are an important tracer for their provenance and tectonic settings (Taylor and McLennan, 1985; McLennan et al., 1993).

The SiO2 and Al2O3 content for the metasedimentary ranges between 66.77 wt% and 13.96 wt%. In Harker's diagrams (**figure 20**), where the SiO2 content was compared with other major elements, it can be observed that the rocks have high contents of Al2O3, FeO, MgO and K2O showing an inverse relationship with SiO2. The relationship it has with TiO2 is a negative but very low trend; With respect to CaO, all the samples except for RC-4 have low contents, finally Na2O is not observed a clear relationship with SiO2.

In the pattern of REE compared with chondrite (McDonough and Sun, 1995) (**Figure 21**) it is characterized by an enrichment in the LREE having a strong slope in all samples except for the sample RC-4 (quartzite), which its slope is a little softer. Together, they all have a depleting in the HREE, with a (La / Yb) N = 6.77 to 10.69 being the RC-4 the one with the highest value and with a well-defined negative anomaly in Eu (Eu / Eu * = 0.46 a 0.68), this refers to the fact that the crust has undergone cortical differentiation dominated by the fractionation of plagioclase; in general, the pattern of the rocks is above 10 in concentration with respect to the normalized primitive mantle

In the multielement diagram normalized with N-MORB (Sun and McDonough, 1989) (**Figure 22**), they are shown to be enriched in LILE, and have poor in HFSE. The graph is characterized by a negative anomaly in Nb, Ta, Hf, and Ti and an enrichment in K, Ba, Rb, Pb and Th.

Th / Sc values commonly track the existence of felsic and / or mafic sources within a sediment. The values obtained are between 0.70 to 1.7 and when compared against Zr / Sc the samples plot close to the upper crust (**Figure 23a**), in the same way in the diagram Hf vs

La / Th (**Figure 23b**) it presents a felsic upper crust signature (Floyd and Leveridge, 1987) and finally in the tectonic discrimination diagram that includes Th-Sc-Zr, the rocks of the Cajamarca Complex plot within the continental island arc field and in the active continental margin field (**Figure 23c**).

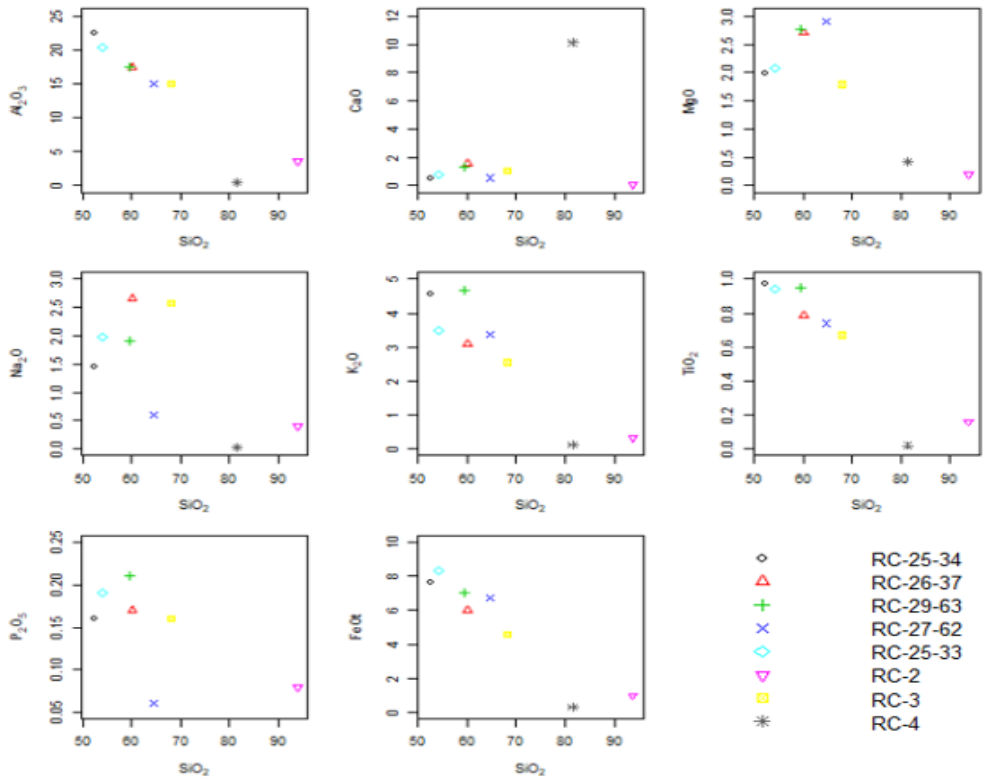

Figure 20 Harker diagrams, major elements vs SiO_2

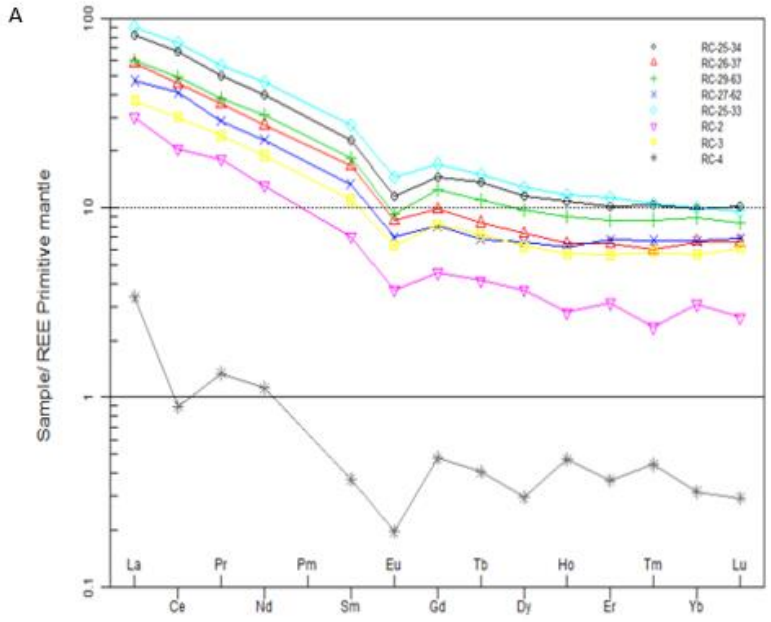

Figure 21. Rare earth elements concentrations normalized with mantle primitive, McDonough and Sun (1995)

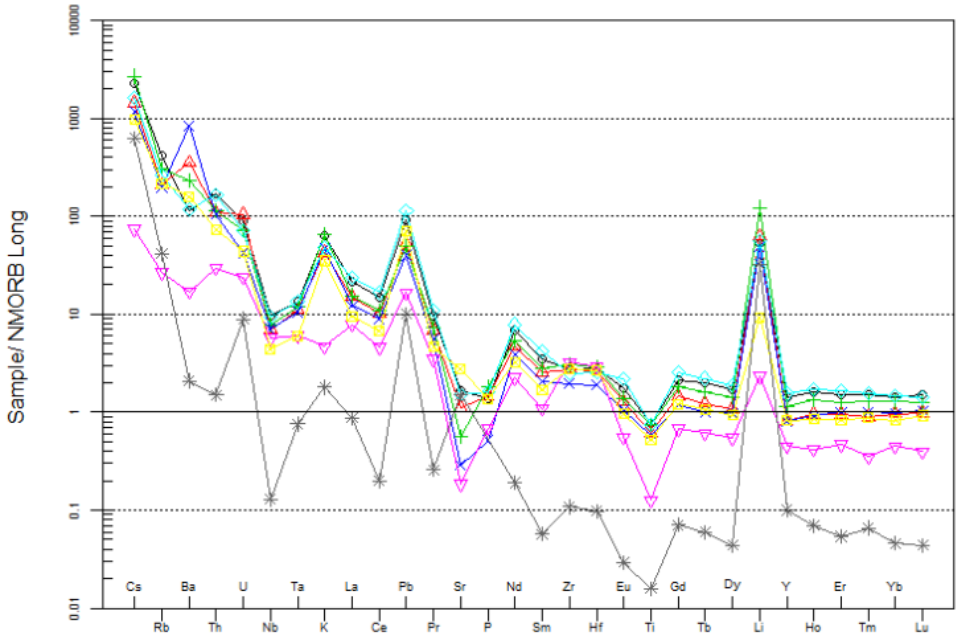

Figure 22. Multi-elemental diagrams normalized to NMORB (Sun and McDonough, 1989)

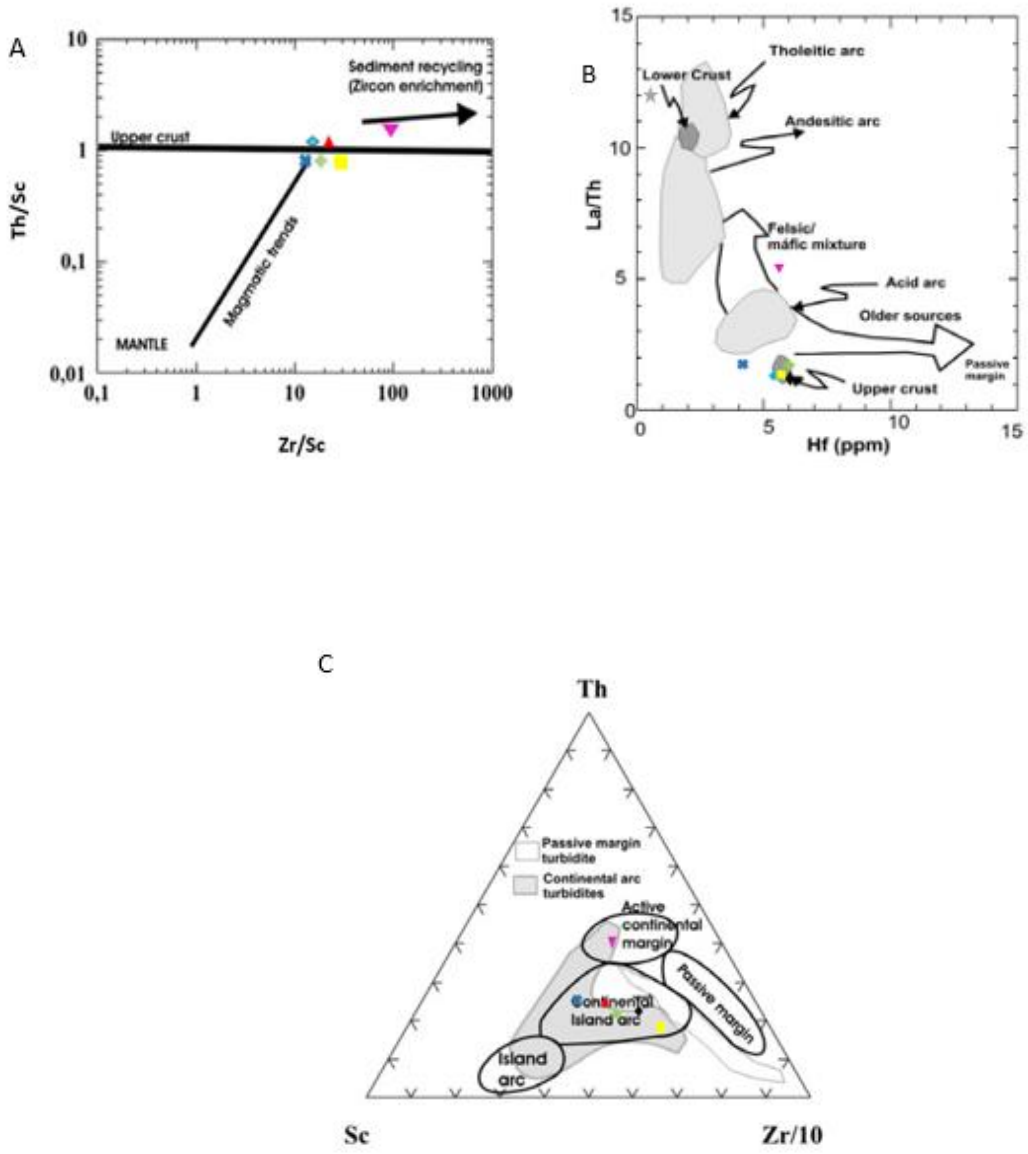

Figure 23. (A). Th/Sc vs Zr/Sc diagram McLennan et al., (1993). (B). Hf vs La/Th (Floyd and Leveridge, 1987). (C). Sandstone geochemical discrimination diagram (Bhatia and Crook, 1986).

6.3.2 Geochemical of metabasic rocks

For the analysis of metabasic rocks, 2 samples (RC1-RC5) were used, as well as for the meta-sedimentary rocks, the HFSE and REE were used for the study due to their immobile nature in metamorphism processes.

The 2 metabasic samples belonging to the Cajamarca Complex (RC1-RC5) present a large variation in the SiO2 content (69.6 and 43.6 wt%), in the same way in the MgO content (2.3 and 7.59 wt%), FeO (5.22 and 16.1 wt%) and CaO (2.99 and 9.5 wt%) with a lower variation of Al2O3 of 13.85 and 14.25 wt%, K2O (0, 65 Y 0.44) and Na2O (3.18 and 2.47).

The Zr / Ti vs Nb / Y diagram marks magma fractionation and alkalinity provides a way to chemically discriminate metamorphosed or altered volcanic rocks (Winchester and Floyd, 1977, Pearce, 1996); in this figure samples RC5 and RC1 plot on basalt and basaltic andesite (**figure 24**)

In the REE pattern compared to the chondrite (McDonough and Sun (1995)) it shows an enrichment in the LREE and a depleting in the HREE (**Figure 25**); La / Yb_N values are 2.61 and 7.45; A negative anomaly in Eu is also shown in both samples (Eu / Eu = 0.66 - 0.89) which refers to the fractionation of palgioclase.

In the normalized multi-element diagram with the primitive mantle (Sun and McDonough, 1989; **Figure 26**), the metabasic rocks show negative slopes, with a slightly flat pattern for the high field strength elements (HFSE), and an enrichment in the large ion lithophile elements (LILE), mainly in Cs, Rb, Ba, K, La and in Pb. Both sections show depletion in Nb, P and Ti.

The Ti and V content of basic magmas often track oxygen activity during magmatic evolution and can therefore be used to identify water-induced melting in subduction environments (Shervais, 1982; Rollinson, 1993), both samples plot in the MORB and Back arc field (**figure**

27). Finally, the graph of Hf-Rb / 30-Ta * 30 (Harris et al., 1986) was made and the samples were plotted on an intraplate (**figure 28**).

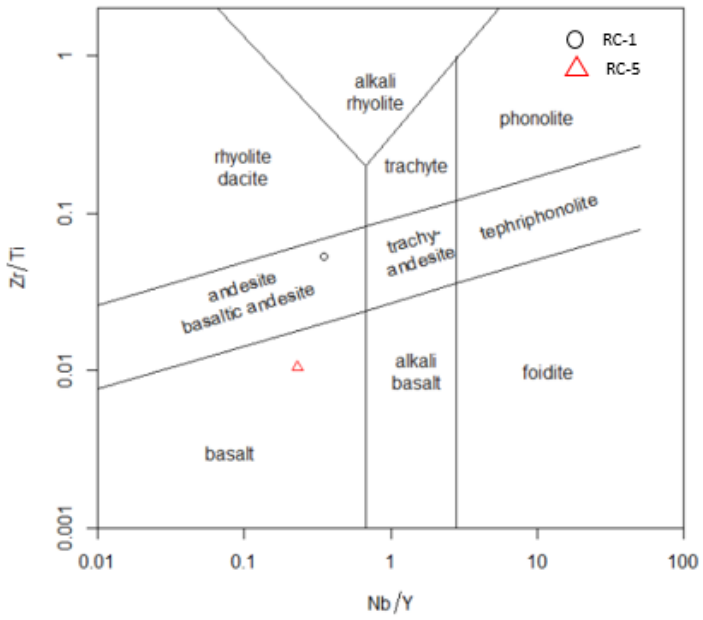

Figure 24 Classification volcanic rocks using inmobile elements (Winchester and Floyd, 1977)

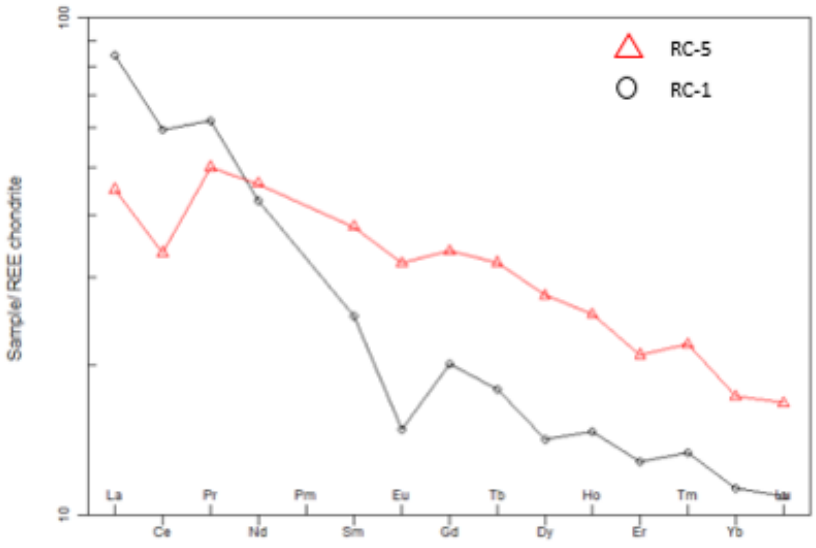

Figure 25. Rare earth elements concentrations normalized to chondrite (McDonough and Sun,1995)

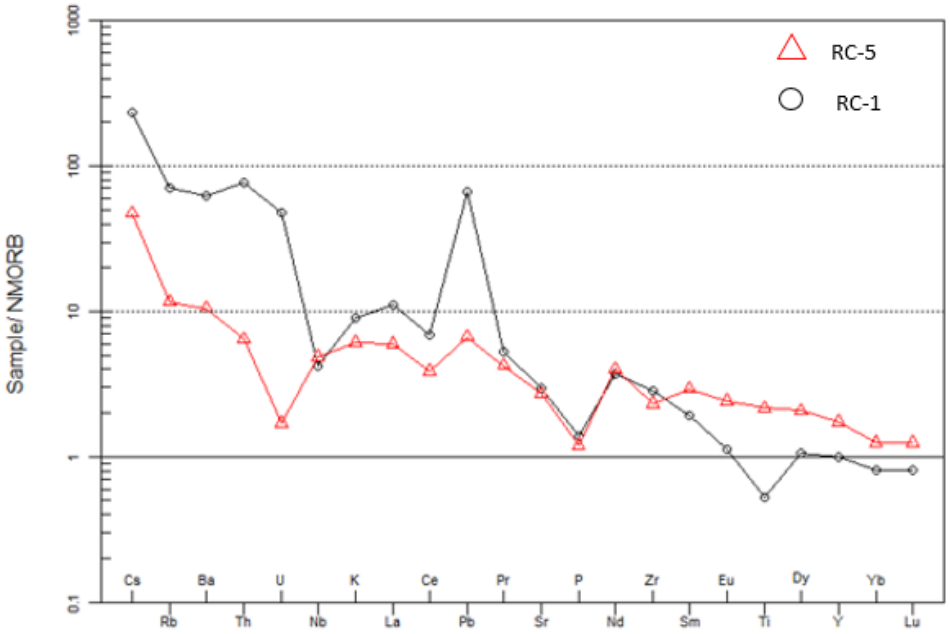

Figure 26. Multi-elemental diagrams normalized to NMORB (Sun and McDonough, 1989)

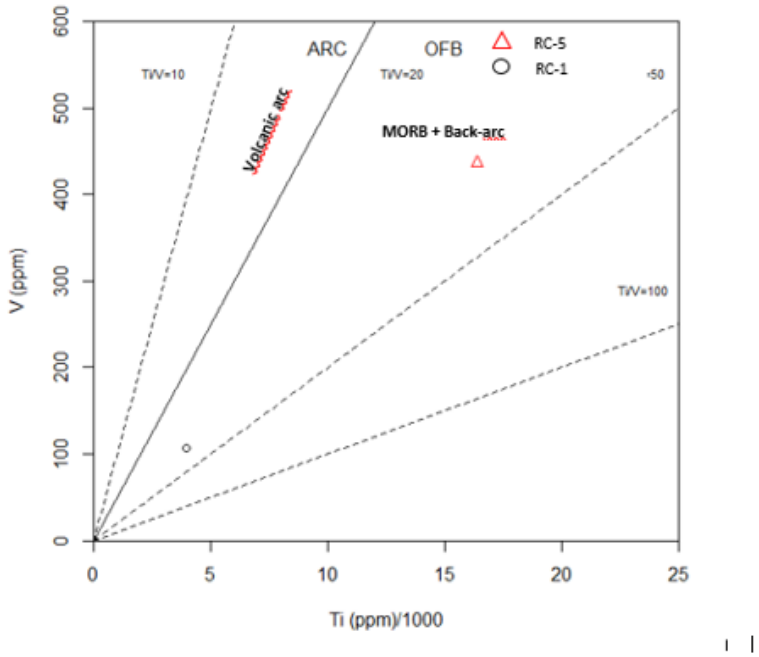

Figure 27. Tectonic setting discrimination diagrams Ti vs V, Shervais (1982)

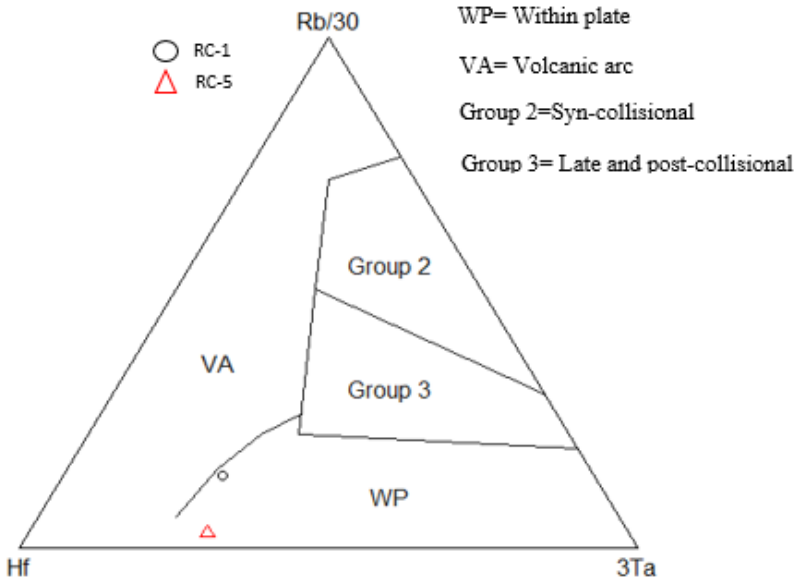

*Figure 28. Hf-Rb/30- Ta*30 diagrams (Harris et al., 1986)*

7 Discussion

7.1 Origin of the protolith

The mineral association, composition and textures of the metasedimentary rocks indicate that the protolith corresponds to continental sediments. This is confirmed in **Figures 23 a and b,** where the samples are plotted in the upper crust. The provenance of the tectonic environment for the protoliths of the metasedimentary rocks, were interpreted from the geochemistry carried out. As can be seen in **figure 23 c**, the samples plot in an active continental margin / continental island arc environment; together with the characteristic anomalies in **figure 22**, such as the negative anomaly of Nb and Ti, the enrichment in Rb, K, Ba which are indicators of a subduction environment.

Blanco Quintero et al. (2014) propose that the protolith of the Cajamarca Complex, near the city of Ibagué, would have accumulated in a deep marine environment, associated with a back-arc basin. Which would have occurred during the early and middle Jurassic. Pulido-Fernández (2017) suggests that the protolith of the metapelites that emerge in the Rio Claro region (Antioquia) and that would be correlated with said Complex (Maya and González, 1995), would be related to a passive continental margin. However, the samples that correspond to the Cajamarca Complex in the work of Pulido-Fernández (2017), graph in the field of an active continental margin, which agrees with the results presented in this work.

For its part, Cediel (2019) proposes an intra-oceanic island arc and a continental margin for the source of the protoliths and proposes two models for the tectonic evolution of the Cajamarca Complex related to the closure of a back-arc basin: 1) an Andean-type margin environment and 2) a continental collision environment, generating a structural reconstruction where it exposes that the formation and metamorphism of the Cajamarca sediments are in an accretion prism that took place in the late Silurian-early Devonian.

The geochemistry results of this work, together with those reported by Pulido-Fernández (2017), allow us to infer that the protolith of the metasedimentary rocks studied in this project would not have accumulated in a back-arc basin environment. On the contrary, its accumulation is associated with an accretion prism of a subduction zone. This can be inferred from the geochemistry of major and trace elements, in which negative anomalies of Nb and Ti, and enrichment of K, Rb and Ba are observed; as well as the relationship of LREE / HREE with $(La / Yb)_N$ between 6.77 and 10.69; which is characteristic of a subduction environment. Additionally, the positive Pb anomaly indicates that the protolith comes from the continental crust.

The metabasic rocks were classified according to the Winchester and Floyd (1977) diagram as basalt and basaltic andesites (**figure 24**). According to the Ti vs V tectonic discrimination diagram, a MORB-like affinity is clearly observed, while the variations observed in Figures 30 and 31 may correspond to the assimilation of sediments or fluid-rock interactions in a subduction zone. According to the above, it can be inferred that the protolith is related to the generation of oceanic crust that would later subduct the paleo-western margin of South America (**figure 32**). Due to the low number of metabasic samples analyzed, it is difficult to be certain of the age of the protolith, and its relationship with the metasedimentary rocks.

7.2 Metamorphic conditions

The metasedimetary rocks of the study area suggest a metamorphism that reaches at least the highest temperatures of greenschist facies, probably epidote-amphibolite facies. This suggest a clockwise path with an approximately isothermic retrograde metamorphism (type ITD) (or isobaric?) but with the petrographic data it is very difficult pinpoint the last portion of the path. It must be considered that part of metamorphism shows evidence of its passage through the reaction chlorite+ K-feldspar ↔biotite + muscovite, in the stability field of andalusite. Due to the absence of minerals typical of metamorphic zones (e.g., garnet, staurolite) there are not practical possibilities to detail the metamorphic path with greater precision for these rocks. So, we suggest that the baric and thermal peaks reached ~0.4 GPa and ~550 °C respectively (**Figure 29**)

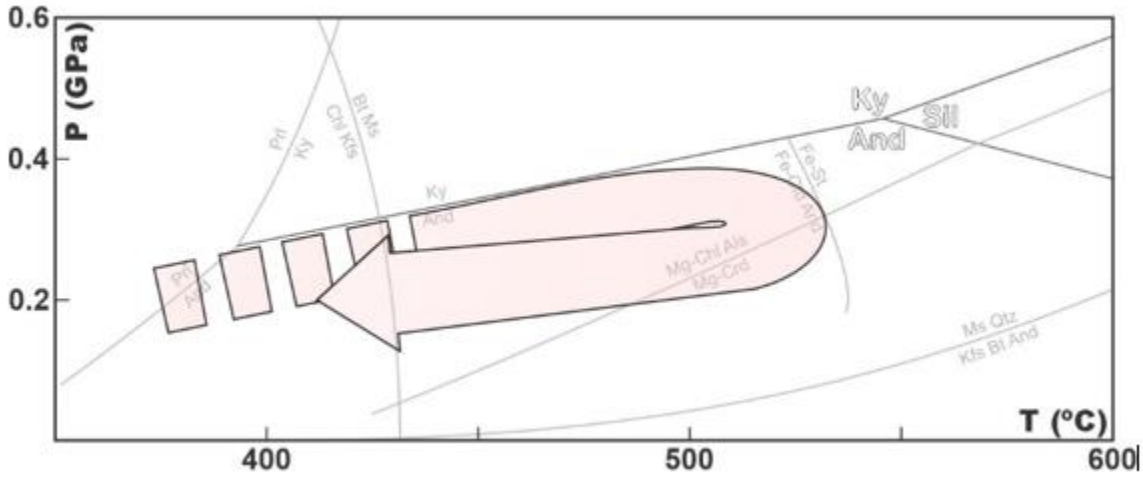

Figure 29. P-T condition of metasedimentary rocks.

In the case of the metabasic rocks studied in this research, due to the relatively monotonous mineralogy that was observed, it becomes more complex to clearly define the metamorphic path followed by these rocks. Considering the paragenesis present in them and represented in the blasthesis diagram, it is possible to suggest that only the epidote comes from a stage prior to the metamorphic peak, possibly from the subgreenschist facies. For another author, the association actinolite+chorite+epidote +albite in presence of quartz changes its stability field under the conditions in which albite becomes calcic and actinolite turns into hornblende and the chlorite disappearance or become unstable at 475°C (e.g., Spear, 1993; Liou et al., 1974), so we use it to determine that the metamorphic peak does not exceed ~550 °C (**figure 30)**, similar conditions to those defined for the meta-sedimentary rocks. The granulometry of these rocks could be used like an indication that they didn't reach higher grades or metamorphic facies (e.g., epidote amphibolite or amphibolite). Due to the association with the meta-sedimentary rocks, a clockwise path, with a retrograde metamorphism is proposed for the metabasic rocks.

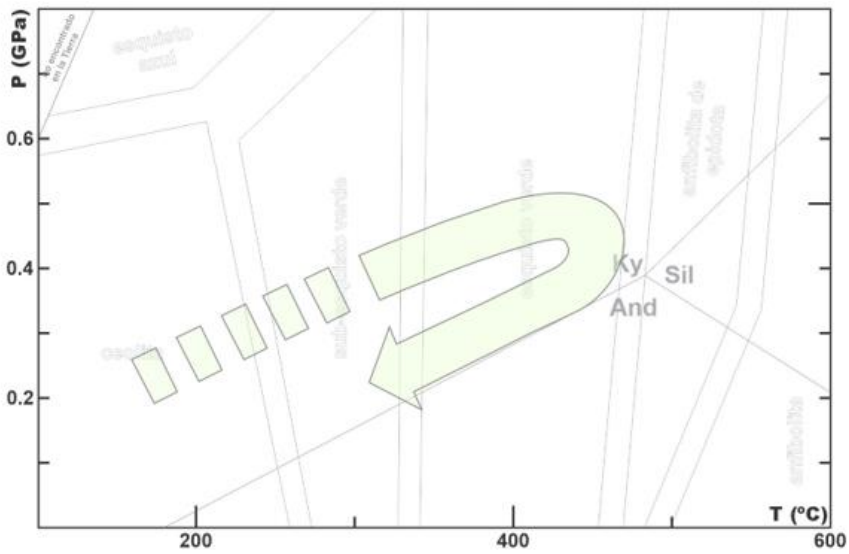

Figure 30. P-T conditions of metabasic rocks

The pressure and temperature conditions for the set of metamorphic rocks were found based on the detailed petrography and the observed metamorphic reactions; the baric and thermal peak for the metasedimentary rocks gave an approximate of 4 Kbar and 550 ° C. In metaigneous rocks, Liou et al., (1974) were taken into account for the baric peak, he estimated under experimental processes the phase relationships between greenschist and amphibolites in basaltic systems; he estimates that the mineralogical association: actinolite + chlorite + epidote + plagioclase + quartz occur in a temperature condition between 350 to 475 ° C, therefore, when applying the textural relationships, he indicates conditions T = 320 - 475 ° C and pressures less than 6 kilobars and the thermal peak in this resource does not exceed 550 ° C, like the metasedimentary; Based on this, depths not exceeding 20 km are indicated during prograde metamorphism (**figure 31**). These conditions would be related to medium P / T series (Barrovian type), generally related to collision systems.

Based on the progressive pattern of the PT paths, which involves burial and heating, the mineralogical assembly, in which the contribution of continental material can be evidenced by the presence of graphite, andalusite concordant with the foliation, a large amount of quartz

in the metasedimentary rocks. and the geochemical results that lead to the accumulation of the protolith possibly in an accretion prism; in addition to that the protoliths of the metabasic rocks were probably formed in an ocean basin; metamorphism could be related to collision and tectonic shortening (**Figure 32**). These conditions of metamorphism are comparable to those described by Blanco-Quintero et al. (2014) for the Cajamarca Complex in the department of Tolima.

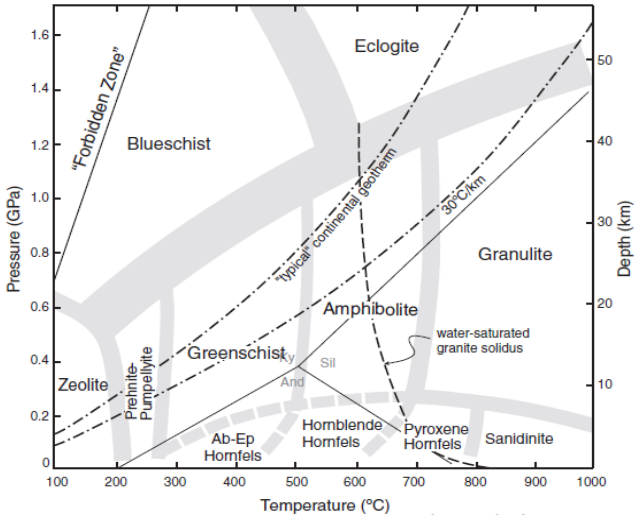

Figure 31. Explicatory diagram relating P-T conditions with tectonic depth (Winter,2014)

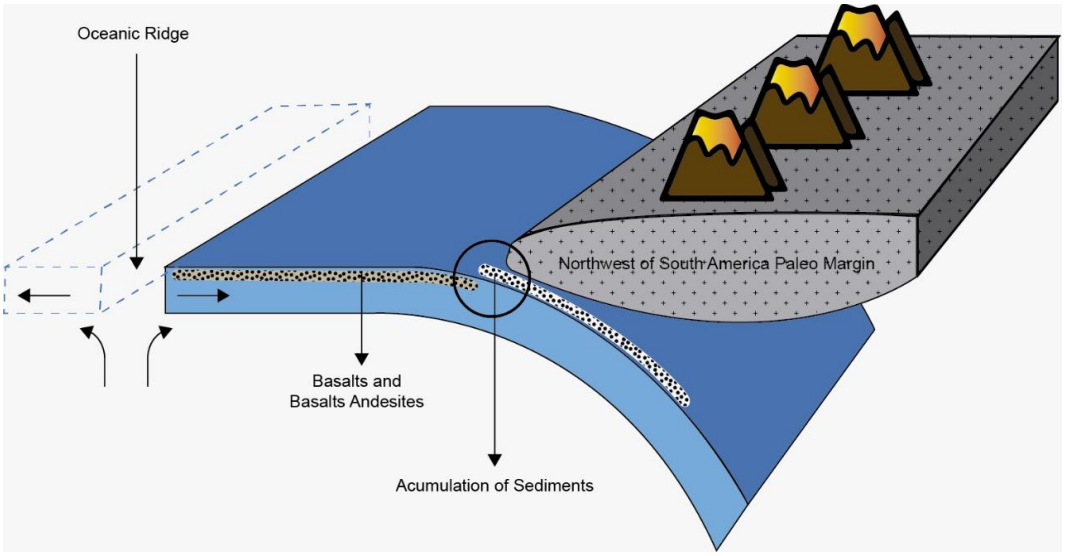

Figure 32. Geological model of the formation of the protoliths and subsequent metamorphism in the subduction zone.

8 Conclusions

Based on the data obtained in this work, a different form of protolith generation is proposed. It is inferred from the geochemical results obtained in the metasedimentary and metabasic rocks, that the protolith of the former would have accumulated in the accretion wedge of a subduction zone, which favors pressure conditions of approximately 4 kbar, this suggests that it was a shallow accumulation and with temperatures that did not exceed 550 ° C, for its part, the igneous protolith as reflected in its results would be part of the oceanic crust that subducts the paleo margin of South America, this would make the protoliths have different ages, obviously the basalts and basalt andesites would have formed in a previous event, as proposed in **figure 32**

As there is no temporality of these samples, it can only be based on the chronology regarding the intrusions and the reported ages of these bodies. These metamorphic rocks are intruded by highly deformed pegmatite bodies, these dikes are closely related to the magmatism of the Antioqueno Batholith, and as is known, it dates from the late Jurassic to the Cretaceous, therefore the metamorphic event had to have been generated during or before the intrusion; which would allow us to compare the metamorphic event with that proposed by Blanco Quintero et al., (2014) south of the Central Cordillera, but the formation of protoliths north of the mountain chain is still under discussion.

It is recommended to carry out more arduous studies in the area, to be able to acquire ages of metamorphism, collect more samples, both in the northern part and in the center, in order to be able to correlate or not with the Cajamarca Complex described to the south and thus be able to better delimit the metamorphic body both temporally and geographically.

9. Acknowledgements

Primero que todo le agradezco a mi asesor Camilo Bustamante Londoño por haberme acompañado en todo el proceso, por haber entendido complicaciones personales y por haberme guiado con sus conocimientos para culminar el trabajo, y por mostrarme día a día que algún día desearía ser como él; también les agradezco a mis amigas Laura Redondo Toro y Daniela Zapata que me alentaban en los días que me estancaba y por ultimo a mi madre Diana María y a mi padre Jhon Madrid que de igual forma estuvieron allí dándome su apoyo incondicional, y a mi amor incondicional Johan Sierra que ha estado en cada paso de este proceso.

9 References

Ardila, R., 1986. Petrografı´a de las rocas metamo´rficas de El Retiro, Antioquia. Monograph. Facultad de Minas, Universidad Nacional de Colombia, Medellın.

Aspden, J.A., McCourt, W.J., and Brook, M., 1987, Geometrical control of subduction-related magmatism: The Mesozoic and Cenozoic plutonic history of Western Colombia: Journal of the Geological Society, v. 144, p. 893–905. doi:10.1144/ gsjgs.144.6.0893

Bard, J.P., 1980. Microtextures of igneous and metamorphic rocks. Universite des Sciences et Techniques du Languedoc, Montpellier. D. Reidel Publishing Company. English edition edited by S. W. Morel.

Bayona, G., Rapalini, A. & Costanzo–Álvarez, V. 2006. Paleomagnetism in Mesozoic rocks of the northern Andes and its implications in Mesozoic tectonics of northwestern South America. Earth, Planets and Space, 58(10): 1255–1272. https://doi. org/10.1186/BF03352621.

Bayona, G., Cardona, A., Jaramillo, C., Mora, A., Montes, C., Valencia, V., Ayala, C., Montenegro, O., and Ibañez, M., 2012, Early Paleogene magmatism in the northern Andes: Insights on the effects of Oceanic Plateau-Continent convergence: Earth and Planetary Science Letters, v. 331–332, p. 97–111. doi: 10.1016/j.epsl.2012.03.015

Bhatia, M., Crook, K.A.W., 1986. Trace element characteristics of greywackes and tectonic setting discrimination of sedimentary basins. Contributions to Mineralogy and Petrology 92, 181–193.

Botero, A. 1941. Formaciones Geológicas de Antioquia. Rev. Min. (Medellín) 111:9080-9085.

Botero, A. 1942. Contribución al conocimiento de la petrografía del Batolito Antioqueño. Rev. Min. (Medellín) 115-117:1318-1330.

Blanco-Quintero, I. F.; García-Casco, A.; Toro, L. M.; Moreno, M.; Ruiz, E. C.; Vinasco, C. J.; Cardona, A.; Lázaro, C.; and Morata, D. 2014. Late Jurassic terrane collision in the northwestern margin of Gondwana (Cajamarca Complex, eastern flank of the Central Cordillera, Colombia). Int. Geol. Rev. 56:1852–1872

Bucher, K;Frey, M. 1994. Petrogenesis of metamorphic rocks. 6th edition. Springer-Verlag Berlin Heidelberg.

Bustamante, C.; Archanjo, C.J.; Cardona, A.; Vervoort, J. D. 2016. Late Jurassic to Early Cretaceous plutonism in the Colombian Andes: A record of long-term arc maturity. Geological Society of America Bulletin 128 (11-12): 1762-1779.

Cardona-Molina, A., Cordani, U.G., MacDonald, W., 2006. Tectonic correlations of pre-mesozoic crust from the northern termination of the Colombian Andes, Caribbean region. Journal of South American Earth Sciences 21, 337–354.

Cardona, A., Valencia, V., Garzón, A., Montes, C., Ojeda, G., Ruiz, J., Weber, M. 2009. Permian to Triassic I to S- type magmatic switch in the northeast Sierra Nevada de Santa Marta and adjacent regions, Colombian Caribbean: Tectonic setting and implications within Pangea paleogeography. Journal of South American Earth Sciences 29 (2010) 772–783.

Cardona, A., Valencia, V., Bustamante, C., García–Casco, A., Ojeda, G., Ruiz, J., Saldarriaga, M. & Weber, M. 2010b. Tectonomagmatic setting and provenance of the Santa Marta Schists, northern Colombia: Insights on the growth and approach of Cretaceous Caribbean oceanic terranes to the South American continent. Journal of South American Earth Sciences, 29(4): 784–804. https://doi.org/10.1016/j.jsames.2009.08.012.

Cediel,F; Shaw, P. 2019.Geoogy and tectonics of Northwestern South America. The pacific Caribbean Andean Junction. Springer.Germany

Cochrane, R., Spikings, R., Gerdes, A., Winkler, W., Ulianov, A., Mora, A. & Chiaradia, M. 2014. Distinguishing between in– situ and accretionary growth of continents along active margins. Lithos, 202–203: 382–394. https://doi.org/10.1016/j. lithos.2014.05.031.

Cordani, U.; Cardona, A.; Jimenez, D. M.; Liu, D.; and Nutman, A. 2005. Geochronology of Proterozoic basement inliers in the Colombian Andes: tectonic history of remnants of a fragmented Grenville belt. Geol. Soc. Lond. Spec. Publ. 246:329–346.

Correa, A., Martens, U., 2000. Caracterizacio´n geológica de las anfibolitas de los alrededores de Medellín. Monograph. Universidad Nacional de Colombia, Medellín.

Correa, M.; Pimentel, M.; Restrepo, J.J.; Nilson, A.; Ordoñez, O.; Martens, U.; Laux, U.; Junges, S. 2006. U-Pb zircon ages and Nd-Sr isotopes of the Altavista stock and the San Diego gabbro: New insights on Cretaceous arc magmatism in the Colombian Andes. In South American Symposium on Isotope Geology, No. 5: 84-86. Montevideo.

Correa, M; Martens, U; Rodriguez,G. 2020. Collage of tectonic slivers abutting the Eastern Romeral Fault System in central Colombia

Duque-Trujillo, J., Bustamante, C., Solari, L., Gómez-Mafla, A., Toro, G., Hoyos, S. 2019. Reviewing the Antioquia batholith and satellite bodies: a record of Late Cretaceous to Eocene syn- to post-collisional arc magmatism in the Central Cordillera of Colombia. Andean Geology 46(1): 82-101. doi: 10.5027/andgeoV46n1-3120

Feininger, T., Barrero, D. & Castro, N. 1972. Geología de parte de los departamentos de Antioquia y Caldas (sub–zona II–B). Boletín Geológico, 20(2): 1–173.

Floyd, P.A., Leveridge, B.E., 1987. Tectonic environment of the Devonian Gramscatho basin, south Cornwall: framework mode and geochemical evidence from turbiditic sandstones. Journal of the Geological Society of London 144, 531–542

González, H. 1980. Geología de las planchas 167 Sonsón y 187 Salamina. Scale 1:100 000. Ingeominas, internal report 1760, 262 p. Medellín.

González, H., Nuñez, A., and Paris, G., 1988, Mapa Geológico de Colombia. Memoria explicativa: Bogotá, Ingeominas.

González, H., 2001. Mapa Geolo´gico del departamento de Antioquia. Escala 1:400.000. Memoria explicativa. Ingeominas, Medellín.

Hall, R.B., Álvarez, J. & Rico, H. 1972. Geología de parte de los departamentos de Antioquia y Caldas (sub–zona II–A). Boletín Geológico, 20(1): 1–85.

Harris, N.W., Pearce, J.A., and Tindle, A.G., 1986, Geochemical characteristics of collision-zone magmatism, in Coward, M.P., and Ries, A.C., eds., Collision Tectonics: Geological Society London Special Publication 19, p. 67–81.

Horton, B.K., Saylor, J.E., Nie, J., Mora, A., Parra, M., Reyes-Harker, A., and Stockli, D.F., 2010, Linking

sedimentation in the northern Andes to basement configuration, Mesozoic extension, and Cenozoic shortening: Evidence from detrital zircon U-Pb ages, Eastern Cordillera, Colombia: Geological Society of America Bulletin, v. 122, no. 9–10, p. 1423–1442.

Hollings, P., Wyman, D., 2005. The geochemistry of trace elements in igneous systems: principles and examples from basaltic systems. In: Linnen, R.L., Samson, I.M. (Eds.), Rare-element Geochemistry and Mineral Deposits:

Geological Association of Canada, GAC Short Course Notes, vol. 17. pp. 1–16.

Hubach, E. 1995. Contribución al conocimiento de las unidades estratigráficas en Colombia. Informe 1212, Bogotá, Serv. Geol. Nal.

Ibáñez-Mejía, M.; Tassinari, C.C.G.; Jaramillo, J.M. 2007. U-Pb zircon ages of the "Antioquian Batholith": Geochronological constraints of late Cretaceous magmatism in the central Andes of Colombia. In Congreso Colombiano de Geología, No. 11. Abstract: 11 p. Paipa.

Janousek, V., Farrow, C.M. and Erban, V. (2006). Interpretation of whole-rock geochemical data in igneous geochemistry: introducing Geochemical Data Toolkit (GCDkit). Journal of Petrology 47: 1,255-1,259.

Jenner, G.A., 1996, Trace element geochemistry of igneous rocks: geochemical nomenclature and analytical geochemistry. In: Wyman, D.A. (Ed.), Trace Element Geochemistry of Volcanic Rocks: Applications for Massive Sulphide Exploration.

Short Course Notes, vol. 12. Geological Association of Canada, pp. 51–77.

Kennan, L. & Pindell, J.L. 2009. Dextral shear, terrane accretion and basin formation in the northern Andes: Best explained by interaction with a Pacific–derived Caribbean Plate? In: James, K.H., Lorente, M.A. & Pindell, J.L. (editors), The origin and evolution of the Caribbean Plate. Geological Society of London, Special Publication 328, p. 487–531. https://doi. org/10.1144/SP328.20

Keppie, J.D., Dostal, J., Murphy, J.B. & Nance, R.D. 2008. Synthesis and tectonic interpretation of the westernmost Paleozoic Variscan orogen in southern Mexico: From rifted Rheic margin to active Pacific margin. Tectonophysics, 461(1–4): 277–290. https://doi.org/10.1016/j.tecto.2008.01.012.

Kerr, A.C., Marriner, G.F., Tarney, J., Nivia, A., Saunders, A.D., Thirlwall, M.F., and Sinton, C.W., 1997, Cretaceous basaltic terranes in western Colombia: Elemental, chronological and Sr–Nd isotopic constraints on petrogenesis: Journal of Petrology, v. 38, p. 677–702. doi:10.1093/petroj/38.6.677
Kroonenberg, S. 1982. A Grenvillian granulite belt in the ColombianAndes and its relations to theGuiana Shield. Geol. Mijnb. 61:325–333.

Kerr, A.C., and Tarney, J., 2005, Tectonic evolution of the Caribbean and northwestern South America: The case for accretion of two Late Cretaceous oceanic plateaus: Geology, v. 33, p. 269–272. doi:10.1130/G21109.1

Kroonenberg, S. 1982. A Grenvillian granulite belt in the ColombianAndes and its relations to theGuiana Shield. Geol. Mijnb. 61:325–333.

Leal-Mejía, H. 2011. Phanerozoic Gold Metallogeny in the Colombian Andes: A Tectono-Magmatic Approach: Ph.D. thesis (Unpublished), Universitat de Barcelona: 1000 p

Liou, J. G., Kuniyoshi, S. and Ito, K. (1974). Experimental studies of the phase relations between greenschist and amphibolite in a basaltic system. American Journal of Science, Vol. 274, pp. 613-632.

Maya, M. & González, H. 1995. Unidades litodémicas en la cordillera Central de Colombia. Boletín Geológico, 35(2–3): 43–57.

McDonough, W.F., and Sun, S.S., 1995, The composition of the earth: Chemical Geology, v. 120, no. 3–4, p. 223–253.

McLennan, S.M., Hemming, S., McDaniel, D.K., Hanson, G.N., 1993. Geochemical approaches to sedimentation, provenance and tectonics. Geological Society of America Special Paper 284, pp. 21–40.

Michard, A., 1989. Rare earth element systematics in hydrothermal fluids. Geochimica et Cosmochimica Acta 53, 745–750.

Moody, J. B., Meyer, D. and Jenkis, J. E. (1983) Experimental characterization of the greens schist – amphibole boundary in mafic systems. American Journal of Science, Vol. 283, pp. 48-92.

Mosquera, D., Núñez, A. & Vesga, C.J. 1982. Mapa geológico preliminar de la plancha 244 Ibagué. Scale 1:100 000. Ingeominas, 27 p. Bogotá

Nance, R.D., Gutiérrez–Alonso, G., Keppie, J.D., Linnemann, U., Murphy, J.B., Quesada, C., Strachan, R.A. & Woodcock, N.H. 2012. A brief history of the Rheic Ocean. Geoscience Frontiers, 3(2): 125–135. https://doi.org/10.1016/j.gsf.2011.11.008

Ospina, Tulio, 1911.- Reseña geológica de Antioquia: Medellín, Imprenta La Organización, 128 p.

Ordóñez-Carmona, O.; Restrepo, J. J.; and Pimentel,M.M. 2006. Geochronological and isotopical review of pre- Devonian crustal basement of the Colombian Andes. J. South Am. Earth Sci. 21:372–382.

Pearce, J.A., Cann, J.R., 1973. Tectonic setting of basic volcanic rocks determined using trace element analyses. Earth and Planetary Science Letters 19, 290–300.

Pearce, J.A., 1982. Trace element characteristics of lavas from destructive plate boundaries. In: Thorpe, R.S. (Ed.), Andesites. John Wiley & Sons, pp. 525–548.

Pearce, J.A., 1996. A user's guide to basalt discrimination basalts. In: En Wyman, D.A. (Ed.), Trace Element Geochemistry of Volcanic Rocks: Applications for Massive Sulphide Exploration. Short Course Notes, vol. 12. Geological Association of Canada, pp. 79–113.

Piraquive, A. 2017. Structural framework, deformation and exhumation of the Santa Marta Schists: Accretion and deformational history of a Caribbean Terrane at the north of the Sierra Nevada

de Santa Marta. Doctorade thesis, Université Grenoble Alpes and Universidad Nacional de Colombia, 393 p. Grenoble–Bogotá

Pulido, N. 2016. Geochemical and petrological characterization of the Cajamarca complex in the Rio Claro area: Metamorphic implications. Undergraduate Thesis for Geosciences. Faculty of sciences Universidad de los Andes

Radelli, Luigi, 1962. Contribution a la geólogie de l'occidente Andin Colombien dans les Departments de Caldas et Antiquia: Travaux de Laboratoire de Geologie de la Faculté des Sciences de Grenoble, v. 41, p. 187-208.

Restrepo-Moreno, S.A.; Foster, D.A.; Kamenov, G.D. 2007. Formation age and magma sources for the Antioqueño and Ovejas batholiths derived from U-Pb dating and Hf isotope analysis of zircon grains. Geological Society of America Progr 39 (6).

Restrepo, J.J. & Toussaint, J.F. 1982. Metamorfismos superpuestos en la cordillera Central de Colombia. V Congreso Latinoamericano de Geología, p. 505–512. Buenos Aires, Argentina. Rodríguez, G., Arango, M.I., Zapata, G. & Bermúdez, J.G. 2014. Petrografía y geoquímica del Neis de Nechí. Boletín de Geología, 36(1): 71–84.

Restrepo, J.J. & Toussaint, J.F. 1988. Terranes and continental accretion in the Colombian Andes. Episodes, 11(3): 189–193.

Restrepo-Pace, P. A.; Ruiz, J.; Gehrels, G.; and Cosca, M. 1997.Geochronology andNd isotopic data of Grenvilleage rocks in the Colombian Andes: new constraints for Late Proterozoic–Early Paleozoic paleocontinental reconstructions of the Americas. Earth Planet. Sci. Lett. 150:427–441.

Restrepo, J., Ordonez Carmona, O., Armstrong, R., 2011. Triassic metamorphism in the northern part of the Tahami Terrane of the central cordillera of Colombia. Journal of South American Earth Sciences 32, 497–507.

Rodríguez, G., Zapata, G., Arango, M.I. & Bermúdez, J.G. 2017. Caracterización petrográfica, geoquímica y geocronología de rocas granitoides pérmicas al occidente de La Plata y Pacarní– Huila, Valle Superior del Magdalena–Colombia. Boletín de Geología, 39(1): 41–68. https://doi.org/10.18273/revbol. v39n1-2017002.

Rollinson, H., 1993. Using Geochemical Data: Evaluation, Presentation, Interpretation. Longman, UK. 352 p.

Sarmiento-Rojas, L. F.; Van Wess, J. D.; and Cloetingh, S. 2006. Mesozoic transtensional basin history of the Eastern Cordillera, Colombian Andes: inferences from tectonic models. J. South Am. Earth Sci.21:383–411, doi:10.1016/j.jsames.2006.07.003

Scheibe, R. 1919. Informe sobre los resultados de la Comisión Cientifica Nacional en Antioquia. Comp. Est. Geol. Of. Col. (Bogotá), 1:67-97.

Shervais, J.W., 1982. Ti–V plots and the petrogenesis of modern and ophiolitic lavas. Earth and Planetary Science Letters 59, 101–118

Spear, F.S. (1993). Metamorphic Phase Equilibria and Pressure-Temperature-

Time Paths. Mineralogical Society of America, Washington, 799 p.

Spikings, R., Cochrane, R., Villagómez, D., van der Lelij, R., Vallejo, C., Winkler, W. & Beate, B. 2015. The geological history of northwestern South America: From Pangaea to the early collision of the Caribbean Large Igneous Province (290–75 Ma). Gondwana Research, 27(1): 95–139. https://doi.org/10.1016/j.gr.2014.06.004

Spikings, R. & Paul, A. 2019. The Permian – Triassic history of magmatic rocks of the northern Andes (Colombia and Ecuador): Supercontinent assembly and disassembly. In: Gómez, J. & Pinilla–Pachon, A.O. (editors), The Geology of Colombia, Volume 2 Mesozoic. Servicio Geológico Colombiano, Publicaciones Geológicas Especiales 36, 42 p. Bogotá. https://doi.org/10.32685/pub.esp.36.2019.01.

Streckeisen, a. (1976). To each plutonic rock its proper name. Earth-Science Reviews, 12(1), 1–33. doi:10.1016/0012-8252(76)90052-0.

Sun, S.S., and McDonough, W.F., 1989, Chemical and isotopic systematics of oceanic basalts; implications for mantle composition and processes, in Saunders, A.D., and Norry, M.J.,

Taylor, S.R., MacLennan, S.M., 1985. The Continental Crust. Blackwell, Oxford. p. 312.

Van der Lelij, R.; Spikings, R.; Ulianov, A.; Chiaradia,M.; andMora, A. 2016. Palaeozoic to Early Jurassic history of the northwestern corner of Gondwana, and implications for the evolution of the Iapetus, Rheic and Pacific Oceans. Gondwana Res. 31:271–294, doi:10.1016/j.gr.2015.01.011.

Villagómez, D., Spikings, R., Magna, T., Kammer, A., Winkler, W., and Beltrán, A., 2011, Geochronology, geochemistry and tectonic evolution of the Western and Central cordilleras of Colombia: Lithos, v. 125, p. 875–896. doi:10.1016/j.lithos.2011.05.003

Vinasco, C.J., Cordani, U.G., González, H., Weber, M. & Peláez, C. 2006. Geochronological, isotopic, and geochemical data from Permo–Triassic granitic gneisses and granitoids of the Colombian central Andes. Journal of South American Earth Sciences, 21(4): 355–371. https://doi.org/10.1016/j.jsames.2006.07.007

Winchester, J.A., Floyd, P.A., 1977. Geochemical discrimination of different magma series and their differentiation products using immobile element. Chemical Geology 20, 325–343

Winter, D., 2014. Principles of igneous and metamorphic petrology. Second edition. Pearson education limited.

Wood, D.A., 1980. The application of the Th–Hf–Ta diagram to problems of tectonomagmatic classification and to establishing the nature of crustal contamination of basaltic lavas of the British Tertiary Volcanic Province. Earth and Planetary Science Letters 50, pp. 11–30.